Dental pulp stem cells

Neurogenic differentiation potential and ferumoxide nanoparticle labelling

Pascal Gervois

promotor :
Prof. dr. Ivo LAMBRICHTS

co-promotor :
De heer Tom STRUYS

Masterproef voorgedragen tot het bekomen van de graad van
master in de biomedische wetenschappen

Universiteit Maastricht

universiteit hasselt

Table of contents

Acknowledgements

Over the last six months, I was able to participate in the stem cell research at the departments of Histology and Morphology at Hasselt University in order to complete my thesis. During these six months, I was learned to be critical, accurate and most importantly, I learned that significant scientific results are based on well coordinated teamwork. Therefore, I would like to thank every person that made it possible for me to do my internship and making these six months a fantastic experience.

First of all I would like to thank my promotor prof. dr. Ivo Lambrichts for his guidance, advice, and valuable yet critical evaluation moments of the performed research. But most of all, I would like to thank him for the kindness and hospitality I experienced during my internship at his department.

I would like to show a lot of gratitude to my co-promotor and daily supervisor Tom Struys for his guidance, recommendations and support during my internship.

Many thanks go out to the rest of the research group: Dr. Annelies Bronckaers and Wendy Martens, thank you for the professional yet amusing guidance.

This internship would not have been possible without external help; therefore my gratitude goes out to Prof. dr. Constantinus Politis of the Ziekenhuis Oost Limburg and faculty of Medicine; Dr. Jules Poukens of the Ziekenhuis Salvator; Prof. dr. Robert Carleer and Mrs. Greet Cuyvers of the department of Applied and Analytical Chemistry; Prof. dr. Uwe Himmelreich and Mrs. Ashwini Atre of the KUL department of Medical Imaging

A word of appreciation goes out to the technical staff for their indispensible assistance: Mrs. Liliane Houbrechts, Mrs. Jeanine Santermans, Mr. Marc Jans, Mr. Hugo Beelen, Mr. Dennis Mathijsen, Mr. Davy Janssen and Mr. Nestor Froidmont.

I thank my fellow students: Kris, Tim, and Petra for the fun during lunch and breaks.

Finally, I would like to thank my parents and my girlfriend for their continuous support during my internship.

Pascal Gervois; June 15th, 2010

List of abbreviations

- AAS Atomic Absorption Spectrophotometry
- ANOVA Analysis Of Variance
- bFGF Basic Fibroblast Growth Factor
- BMMSC Bone Marrow Derived Mesenchymal Stem Cell
- DPSC Dental Pulp Stem Cell
- EGF Epidermal Growth Factor
- FACS Fluorescence-Activated Cell Sorting
- FCS Fetal Calf Serum
- FITC Fluorescein Isothiocyanate
- GalC Galactosylceramidase
- GFAP Glial Fibrillary Acid Protein
- HSC Hematopoietic Stem Cell
- ICC Immunocytochemistry
- LM Light Microscopy
- MPIO Micron Sized Paramagnetic Iron Oxide Particles
- MRI Magnetic Resonance Imaging
- MSC Mesenchymal Stem Cell
- MTT 3-(4,5-Dimethylthiazol-2-yl)-2,5- Diphenyltetrazolium Bromide
- NCAM Neural Cell Adhesion Molecule
- NeuN Neuronal Nuclei
- NGFRp75 Nerve Growth Factor Receptor p75
- NSC Neural Stem Cell
- NSE Neuron Specific Enolase
- PBS Phosphate Buffered Saline
- PGP9.5 Protein Gene Product 9.5
- PLL Poly-L-Lysine
- ROS Reactive Oxygen Species
- SPIO Superparamagnetic Iron Oxide Particles
- TEM Transmission Electron Microscopy
- USPIO Ultrasmall Superparamagnetic Iron Oxide Particles

Abstract

Introduction: Dental pulp stem cells (DPSC), mesenchymal stem cells (MSC) from the tooth, share phenotypical and multilineage characteristics with bone marrow derived MSCs (BMMSCs). Since DPSCs are much easier to harvest in comparison to BMMSCs it is worthwhile to consider them as a useful alternative MSC source in stem cell research. As some studies show that MSCs retain some plasticity, the neural differentiation potential of DPSCs will be evaluated. Furthermore, the baseline expression of neural related markers will be compared between DPSCs and BMMSCs. DPSCs will be labelled with the commercially available ferumoxide Endorem® to allow visualization with MRI following engraftment.

Materials and methods: DPSCs were isolated from extracted third molars with informed consent of the patient. These cells were then induced towards neurogenic differentiation or were labelled with different concentrations of Endorem® whether or not combined with Poly-L-Lysine (PLL). Differentiated cells were subjected to an immunocytochemical analysis testing general neural associated markers and TEM analysis. Labelled cells were subjected to MRI and TEM analysis. Cell viability and intracellular iron content were determined using MTT and atomic absorption spectrophotometry (AAS) respectively.

Results: Both DPSCs and BMMSCs show baseline expression of neural associated markers. Only NeuN was found to be differentially expressed in induced DPSCs. Ultrastructurally, differentiated cells acquire a bipolar morphology and an increased metabolic activity. Vesicular transport was observed at cell-cell contact zones between differentiated cells. MRI, MTT, AAS and TEM analysis showed that DPSCs could be labelled with Endorem® when combined with PLL, preserving cell viability and morphology. Labelling cells prior to neurogenic differentiation did not influence neurosphere formation and outgrowth. TEM analysis showed that Endorem® is homogeneously distributed in endosomes and the cells appear bipolar. Differentiated labelled cells did not show reactivity for NeuN.

Discussion: This study shows the need of a specific marker for neurogenic differentiated cells as DPSCs and BMMSCs show baseline expression of conventionally used markers. This study proposes NeuN as such a marker. Future studies should include quantitative and electrophysiological experiments. This study also shows that the optimal concentration for labelling DPSCs is 0,75µg/ml PLL with 15µg/ml Endorem®. The influence of Endorem® labelling on the differentiation potential of DPSCs needs to be determined before these cells can be considered as a clinical applicable intracellular contrast agent for MRI analysis.

Samenvatting

Introductie: Dentale pulpastamcellen (DPSC), mesenchymale stamcellen (MSCs) uit de dentale pulpa, delen fenotypische- en meerdere lijnsdifferentiatie eigenschappen met MSCs uit het beenmerg (BMMSCs). Aangezien DPSCs makkelijker te isoleren zijn dan BMMSCs, worden ze beschouwd als een waardevol alternatief voor BMMSCs in stamcelonderzoek. Omdat werd aangetoond dat mesenchymale stamcellen enige plasticiteit bewaren zal het neurogene differentiatiepotentieel van DPSCs onderzocht worden. Daarenboven wordt de basale expressie van neuraal-gerelateerde merkers vergeleken tussen DPSCs en BMMSCs. DPSCs worden gelabeld met het commercieel beschikbare ferumoxide Endorem® met als doel deze cellen te kunnen visualiseren met MRI na transplantatie.

Materiaal en methoden: DPSCs werden geïsoleerd uit chirurgisch verwijderde derde molaren met toestemming van de patiënt. Deze cellen werden nadien neuraal gedifferentieerd, of ze werden gelabeld met verschillende concentraties Endorem® al dan niet gecombineerd met Poly-L-Lysine (PLL). Gedifferentieerde cellen werden geëvalueerd met immunocytochemie voor de aanwezigheid van algemene neurale merkers en met transmissie electronenmicroscopie (TEM). Gelabelde DPSCs werden geëvalueerd met TEM en MRI of werden verwerkt om celviabiliteit na te gaan met een MTT assay of de intracellulaire inhoud te bepalen met atomische absorptiespectrometrie (AAS).

Resultaten: Zowel DPSCs als BMMSCs vertonen basale expressie van neuraal-geassocieerde merkers. Enkel NeuN kwam differentieel tot expressie in geïnduceerde DPSCs. Ultrastructureel verwerven gedifferentieerde DPSCs een bipolaire morfologie en een verhoogde metabole activiteit. Vesicular transport werd waargenomen aan cel-cel contactzones tussen gedifferentieerde cellen. MRI, MTT, AAS en TEM analyses tonen aan dat DPSCs gelabeld kunnen worden met Endorem® in combinatie met PLL terwijl celviabiliteit en morfologie behouden blijven. De ijzerdeeltjes zijn homogeen verdeeld in intracellulaire endosomen. Cellabelling voor neurogene differentiatie werd ingezet, had geen invloed op neurosfeervorming en celuitgroei. Immunoreactiviteit voor NeuN kon echter niet worden waargenomen. Ultrastructureel zijn de Endorem® deeltjes homogeen verdeeld in endosomen. De cellen zijn bipolair en de celmorfologie werd bewaard.

Discussie: Deze studie toont aan dat er een nood is aan specifieke merkers voor neurogeen gedifferentieerde cellen aangezien zowel DPSCs als BMMSCs basale expressie vertonen van neuraal geassocieerde merkers. NeuN wordt voorgesteld als een geschikte merker. Verdere studies dienen zich toe te spitsen op kwantitatieve en elektrofysiologische experimenten. Deze studie toont ook aan dat de optimale labellingsconcentratie voor DPSCs bestaat uit 0,75µg/ml PLL met 15µg/ml Endorem®. De invloed van PLL/Endorem® labelling op het differentiatiepotentieel van DPSCs dient echter bepaald te worden voordat deze als klinisch toepasbaar intracellulair contrastagens beschouwd kan worden voor MRI analyses.

1 Introduction

One of the greatest medical breakthroughs of the twentieth century was the discovery of stem cells. These are defined as clonogenic cells with the ability to self-renew and the potency to differentiate into different cell types. Stem cells are therefore considered as a potential treatment for degenerative diseases, being able to replace the damaged tissue. Three types of stem cells have been defined, based on their capacity to differentiate into different cell types or -lineages. Totipotent stem cells have the ability to develop into an entire organism, including all extraembryonic tissue. In animals, totipotent stem cells can be isolated from the zygote and the morula. Pluripotent stem cells are capable of developing into all types of cells and tissues that arise from the three germ layers: ectoderm, endoderm and mesoderm. However, these cells cannot develop into an entire organism by itself caused by the inability to differentiate into extraembryonic tissue. Pluripotent stem cells can be found in the inner cell mass of the blastocyst. The third type of stem cell is the multipotent stem cell. These cells include postnatal or adult stem cells with the capability of multilineage differentiation, generally committed to one germ layer. Multipotent stem cells can be subdivided into three major classes: neural stem cells (NSC), hematopoietic stem cells (HSC), and mesenchymal stem cells (MSC) [1, 2].

Impeded by ethical considerations regarding the use of pluripotent embryonic stem cells, research groups are in search of a suitable alternative to gain access to stem cell material. Therefore, stem cell sources that can be readily harvested from adult individuals seem to be a promising alternative. The general aim of research groups focusing on stem cells is to develop a stem cell based therapy for various disorders. Depending on the intended therapy, different types of multipotent stem cells can be applied. For example, HSC are currently being used for nearly three decades to treat blood cancers while MSC therapy is considered for instance in treating bone diseases, recovery after heart failure, liver diseases and cartilage replacement in damaged joints [3, 4]. This raises the question whether NSC can be used for disorders affecting the nervous system [5]. Unfortunately, human experiments with autologous NSC are challenging to perform due to the scarce amount of NSC in the adult brain while also being difficult to harvest. Therefore, the search for an alternative source of stem cells with neural differentiation potential is an open challenge [6]. It has already been shown that MSC retain some plasticity to transdifferentiate to cells from another germ layer and more specifically to neural cells derived from the ectoderm [2, 7]. Stem cells are also considered as a therapeutic option based on their immunomodulatory capacities and the release of specific molecules

influencing the micro-environment of the target tissue. Among the proposed mechanisms of MSC immunomodulation, suppression of T cell and natural killer cell proliferation, inhibition of dendritic cell differentiation and modulation of B cell function by either the release of interleukins or direct cell-cell contact have been proposed. However, due to contradicting *in vitro* results, these mechanisms need to be clarified. Furthermore, the biological relevance of immunomodulatory properties of MSC has yet to be shown [8].

1.1 Dental pulp stem cells: MSCs from the human dental pulp

MSCs, firstly isolated from human bone marrow, are found to be present in the stroma of almost every adult organ in the human body, including teeth, the umbilical cord, trabecular bone and adipose tissue [9-12]. The presence of MSCs in various easily accessible organs makes this type of stem cell a promising cell type for stem cell based therapies. However, one of the main problems in the extensive research with MSCs, is the difficulty to compare study outcomes between different research groups. Research groups often have their own methods of isolating, expanding and characterizing the cells, leading to diverging criteria to define MSCs.

After the discovery of MSCs in human dental pulp (DPSCs), various applications of these cells came into mind. In the adult teeth, DPSCs are activated after severe injury caused by mechanical trauma and dentinal degradation by bacteria. Severe damage to the tooth, requires reparative dentinogenesis in which new dentin-secreting odontoblasts are formed out of DPSCS [13]. A study by Gronthos et al. showed that DPSCs were able to form dentin both *in vitro* and following transplantation into immunocompromised mice. Therefore, DPSCs were firstly isolated and expanded, considering possible applications in tooth engineering. Subsequent studies compared DPSCs with bone marrow derived MSCs (BMMSCs), the most extensively studied MSC. Immunophenotypical analysis of DPSCs and BMMSCs showed a comparable set of surface markers. Furthermore, it was shown that DPSCs were plastic adherent under standard culture conditions and were able to differentiate into classical mesodermal cell lineages, forming adipocytes, chondroblasts and osteoblasts in vitro [10, 14, 15]. In addition, DPSCs showed a higher proliferative rate than BMMSCs. Comparing DPSCs and BMMSCs by cDNA microarray analysis aimed to provide additional information of both cell types. Over 4000 known human genes were found to have a similar expression level in both human DPSCs and BMMSCs [16]. Another argument that favours DPSCs as a suitable alternative for BMMSCs, is the ease in which they can be harvested. DPSCs can be isolated

from dental pulp from extracted teeth, whilst BMMSCs need to be isolated from bone marrow aspirates with a higher chance of donor site morbidity.

1.1.1 DPSCs as an alternative source in treating neurodegenerative diseases

Using DPSCs as an alternative for BMMSC in stem cell research, several research groups focussed on the differentiation capacities of DPSCs. As mentioned, DPSCs are able to differentiate into adipocytes, osteoblasts and chondroblasts. In addition, several studies focussed on the plasticity of DPSCs to transdifferentiate to neural-like cells. A study by Sasaki et al. describes the ability of rat DPSCs to undergo transdifferentiation and generate neurospheres *in vitro*, while a study by Stevens et al. describes sphere forming abilities of human DPSC [17, 18]. This indicates that DPSCs maintain some form of plasticity, being potentially able to differentiate into neural tissue which is derived from the ectoderm. During embryogenesis, cells migrate from the neural crest to the region of the mesenchyme that will later contribute to the development of the head and the neck. In this region, tooth germs are formed which will later differentiate into dental structures, including the dental pulp. As a result, dental tissue is composed of both neural crest derived mesoderm (ectomesenchym) and other mesenchymal components [19]. Electrophysiological studies of differentiated DPSCs showed that DPSCs can differentiate towards functionally active neurons producing a sodium and potassium current when cultured in appropriate neuronal inductive growth media [20, 21]. Based on the observations that DPSCs retain some plasticity and can differentiate towards functional neurons, these cells might have an application in stem cell based therapy for disorders in the central nervous system. These could either be neurodegenerative or autoimmune disorders. Since autologous NSC therapy in particular proves to be difficult, DPSCs might be a useful alternative for NSC in stem cell based therapy. When rat DPSCs are cultured with trigeminal neurons they promote neurite outgrowth and cell survival. This effect was attributed to the production of neurotrophic factors including nerve growth factor, brain-derived neurotrophic factor and glial cell-line derived neurotrophic factor. This neurotrophic effect was also observed in a rat model for spinal cord injury where grafting DPSCs increased the number of surviving motoneurons. The latter indicating a functional neuroprotective activity of the dental pulp derived neurotrophic factors [22]. Recent studies have shown that human DPSCs also secrete these neurotrophic factors *in vitro* [23]. Another study has shown that in *in vitro* models of Alzheimer's and Parkinson's disease, rat DPSCs have a neuroprotective effect in primary neurons [24]. In support of these results, rat DPSCs were

also shown to promote the survival of dopaminergic neurons *in vitro*. Furthermore, it was shown that DPSCs survived when grafted in a neural environment and that a fraction of cultured DPSCs, both of human and rat origin, differentiate and maintain a neural phenotype and morphology. Cultured cells showed a round cell body with several neurites and were positive for the neural markers protein gene product 9.5 (PGP9.5) and beta-III tubulin [23]. In another study, DPSCs obtained from rhesus monkeys were engrafted into the hippocampus of immunosuppressed mice. This resulted in the proliferation of endogenous neural cells and the recruitment of pre-existing neural progenitor cells and mature neurons to the site of engraftment. The graft promotes growth factor signalling, increasing the expression of ciliary neurotrophic factor, vascular endothelial growth factor and fibroblast growth factor [25]. Together, these results suggest that DPSCs can promote the survival of different subsets of neurons and are able to promote proliferation and maturation of endogenous progenitor- and stem cells. Furthermore, DPSCs can adapt a neural-like morphology and phenotype in culture. The rationale behind using DPSCs as a potential stem cell source in treating disorders of the nervous system is therefore two-fold. On the one hand, there are indications that differentiated DPSCs have a neurotrophic effect by the release of neurotrophic factors. On the other hand, tissue repair by engrafting functionally active neurons is another approach for DPSC transplantation in neurodegenerative disorders. However, most research that was performed used animal models or cell cultures for their *in vitro* or *in vivo* experimentss, rendering extrapolation of these results to human applications a question that needs to be addressed.

1.1.2 Neural crest derived DPSC niche in the dental pulp

The dental pulp is comprised of a heterogeneous group of cells with less than 1% of the total cell population in the dental pulp being DPSCs. Studies attempting to elucidate the location of stem cell niches in the pulp have proposed that the cells can reside in the pulpal stroma, form a perivascular cell population or can be found in the cell-rich layer in the proximity of the existing post-mitotic odontoblasts [26]. Given the heterogeneity of the cell population in the dental pulp, there is need of a marker that is able to isolate the stem cell fraction from the other cells in the dental pulp. Subsets of perivascular MSCs, including BMMSCs, MSCs in adipose tissue and DPSCs have been isolated using Stro-1 as a surface marker. Furthermore, the Stro-1 sorted DPSCs (+/-6%) were positive for the vascular associated cell marker CD146, and the pericyte-associated antigen 3G5. These cells were also shown to be negative for the HSC marker CD34. This suggests that Stro-1 sorted DPSCs might origin from the

perivascular stem cell niche [27-29]. In addition, sorting Stro-1 positive cells from the other cells in the rat dental pulp, led to the observation that these cells were more capable of differentiating towards multilineage cell types compared to non-sorted cells as determined by Light microscopy, histochemistry and immunocytochemistry [30].

Given the predisposition of neural crest derived cells to neural cells in embryonic development, the question arises whether there is a fraction of stem cells in the tooth that still retains some characteristics of neural-crest like cells. Nerve growth factor receptor p75 (NGFRp75) has been shown to be a marker for neural crest derived stem cells [31]. Studies using rat DPSCs identified a subpopulation of DPSCs derived from the neural crest, showing high expression of NGFRp75 [32, 33]. Furthermore these cells were positive for Stro-1, proposing that the isolated cells have a better multilineage differentiation capacity compared to the subset of Stro-1 negative cells that reside in the dental pulp. It is important to note that the NGFRp75 positive cells only constitute a small fraction of the isolated DPSCs (<0,01%) as determined by magnetic activated cell sorting, but that these cells were all Stro-1 positive. These results suggest that the perivascular subpopulation of DPSCs is Stro-1 positive and a subset of these cells is NGFRp75 positive, based on the expression of endothelial, pericyte and vascular associated markers [33].

1.2 Magnetic resonance imaging of stem cells using ferumoxide nanoparticles

In order to evaluate the possible clinical use of DPSCs, it is necessary to map the migration pathways of these cells following engraftment. Preferably non-invasive imaging techniques are used to monitor *in vivo* stem cell behaviour. Histological analysis can give detailed information of stem cells after transplantation, but the required invasive techniques often lead to damage to the host or even death during sample preparation. Another drawback of using invasive methods to monitor stem cell behaviour is that it is unable to give spatio-temporal information of the engrafted cells. Magnetic Resonance Imaging (MRI) is a non-invasive imaging method depending on the magnetic relaxation properties of hydrogen atoms oriented according to an externally applied magnetic field. After disturbing the magnetic orientation of the hydrogen atoms by radiofrequency pulses, their magnetic relaxation profile can be used to gain a detailed image of the tissue of interest. These magnetic relaxation properties depend on the way hydrogen atoms are incorporated into biochemical structures. Based on the measurement settings, two different relaxation profiles can be obtained. In T1 weighted images loosely bound hydrogen atoms have a low signal intensity while structured hydrogen

atoms cause a high signal intensity. In T2 weighted images, loosely bound hydrogen atoms are clearly visualized while more structured hydrogen atoms show a low signal intensity [34].
A contrast agent is frequently used in MRI to label the exogenous cells in order to distinguish between the host and transplanted cells. Iron oxide based nanoparticles have already shown their potential in labelling stem cells. These, or other metal based contrast agents are able to disturb the generated magnetic field, thereby decreasing the relative signal intensity in T2 weighted images. In these images, the contrast agent will appear as a hypointense signal. Several different iron oxide based nanoparticles are available: superparamagnetic iron oxide particles (SPIO), micron sized paramagnetic iron oxide particles (MPIO) and ultrasmall superparamagnetic iron oxide particles (USPIO). The larger particles like SPIOs and MPIOs have been shown to be more easily endocytosed than USPIOs [35]. Among the SPIOs, ferumoxides like Feridex® and Endorem® are FDA approved as a contrast agent for liver magnetic resonance images (Feridex®-USA; Endorem®-Europe). Furthermore, these SPIOs have shown great potential in *in vitro*- and animal model studies of cell-labelling. Using ferumoxides as a cell-labelling agent for MRI, has led to the labelling of a variety of cells, including MSCs and NSCs [36-38]. Dextran coated SPIOs show excellent biocompatibility and are frequently modified with poly-l-lysine (PLL) to improve cellular uptake. Mixing anionic dextran-coated SPIOs with cationic charged PLL leads to electrostatic alterations in the interaction between the cell membrane and the surface of the SPIO. As a result of these changes, an increased internalization of the SPIO-PLL complexes is observed [38, 39]. A study by Yocum et al. showed that SPIO-PLL labelled human MSCs do not clinically alter biochemical or hematologic organ functions after injection into immunodeficient mice [40]. Furthermore MSC are traceable with MRI after labelling them with SPIOs while preserving multilineage MSC differentiation with subtle but significant phenotypical changes [41].

1.3 Research aims and experimental setup

This study hypothesizes that DPSCs can differentiate to neural cells, and that these cells can also be labelled with Endorem®, present as a homogeneously distributed endosomal intracellular agent while preserving cell viability and morphology. In first instance, the MSC phenotype will be determined by the markers vimentin, CD29, CD44, CD105, CD146, CD34 and c-kit. CD34 serves as a negative control marker, being restricted to HSCs while vimentin, CD29, CD44, CD105 and CD146 are used as positive controls. C-kit is a general stem cell marker. Nestin will be used as a marker to evaluate basal NSC characteristics of DPSC as

nestin is most frequently used as a marker for NSCs or neural precursor cells. Next, Fluorescence activated cell sorting (FACS) will be used to determine whether the applied cell population is in consent with the one described in literature, based on the expression level of NGFRp75 and Stro-1. In subsequent experiments, DPSCs will be differentiated using basic fibroblast growth factor (bFGF) and epidermal growth factor (EGF) as neural inducing media. The differentiated cells will be evaluated at the ultrastructural level by means of transmission electron microscopy (TEM). This evaluation will be based on the presence or absence of neuron characteristics such as dendritic processes, the formation of synapses with other neurons and accumulation of intracellular vesicles. The expression of neural associated markers in differentiated and undifferentiated cells will be investigated by immunocytochemistry (ICC). These markers include beta-III tubulin, neurofilament, S-100, synaptophysin, neuron specific enolase (NSE), galactosylceramidase (GalC), A2B5, glial fibrillary acid protein (GFAP), PGP9.5, neural cell adhesion molecule (NCAM), NGFRp75 and neuronal nuclei (NeuN). Neurofilament is a general marker for neural cells while beta-III tubulin and NeuN are used to distinguish between early-intermediary and maturated neurons respectively. Synaptophysin is a marker for presynaptic vesicles, whereas S-100 is a cytoskeletal marker that stains neural crest derived cells, adipocytes and chrondocytes amongst others. NSE and GalC are enzymes present in cells of neuronal origin, the latter also being expressed in myelin producing cells. NGFRp75 is a neurotrophin receptor that binds to most neurotrophins while NCAM is an adhesion molecule that is expressed on different cell types, including neurons and glial cells. PGP9.5 is a neuron specific protein and A2B5 is an epitope present on neural progenitor cells. Preliminary results show that exposing DPSCs to bFGF as an inducing agent leads to drastic morphological changes in the cell. Bipolar cells with very thin cytoplasmic extensions and intracellular accumulation of vesicles were observed using TEM. Furthermore, these cells were positive for beta-III tubulin. In a pilot experiment, the basal expression of neural markers on BMMSCs will be evaluated to assess potential neural predisposition of DPSCs compared to BMMSCs. This part of the study aims to find differential expression levels of neural related markers between undifferentiated and differentiated DPSCs in addition to morphological changes as determined by TEM.

The efficiency of Endorem® in labelling stem cells will be evaluated by using different ratios of Endorem® and PLL to determine the optimal labelling concentration. In first instance, MRI phantoms will be constructed with the different labelling conditions to verify if the labelled

cells can be visualized with MRI both one day and three days after labelling. Next, an ultrastructural evaluation will be performed for those labelling conditions that have suggested to be efficient in labelling DPSCs, based on the results of the MRI images one day and three days after labelling. At the ultrastructural level, cell morphology following cell labelling is assessed together with the intracellular distribution of the particles. Criteria include the integrity of the intracellular organelles and both the cell- and nuclear membrane. Whether the particles appear as clustered units or as a homogeneously distributed substance in endosomes, is another criterion in evaluating cell labelling at the ultrastructural level. Next, cell viability/metabolic activity and intracellular iron content will be assessed for those labelling conditions that demonstrate to be most suitable for DPSC labelling. Cell viability/metabolic activity will be evaluated three days after labelling with a 3-(4,5-Dimethylthiazol-2-Yl)-2,5-diphenyltetrazolium bromide (MTT) assay. Subesquently, the amount of iron that is present in the cell after endocytosis will be quantified using Atomic Absorption Spectrophotometry (AAS) three days after labelling the cells. This part of the study will determine the optimal labelling concentration of PLL/Endorem® in DPSCs.
In another pilot experiment, the influence of PLL/Endorem® labelling on neurogenic differentiation will be evaluated. These experiments include the ability of labelled cells to form neurospheres *in vitro* and an ultrastrucural evaluation of labelled, differentiated DPSCs. Furthermore, an ICC analysis for neurogenic markers that have proven to be differentially expressed in neurogenic differentiated cells compared to non-differentiated DPSCs will be performed.

This study will provide more insight into the neural differentiation capacity of DPSC by focusing on the ultrastructural appearance of differentiated DPSCs and the expression of several neural-associated markers as determined by ICC. In addition, the baseline expression of neural associated markers will be compared between BMMSCs and DPSCs. Furthermore, the ability of DPSCs to be labelled with Endorem® is assessed together with a determination of the optimal labelling concentration, evaluating the potential use of this stem cell type in cell-imaging research. Finally, primary tests will evaluate the ability of labelling neurogenic differentiating DPSCs with Endorem®.

2 Materials and methods

In order to evaluate the DPSCs or BMMSCs, the cells needed to be maintained in culture before any differentiation or labelling experiments could be performed. Afterwards, samples were prepared for transmission electron microscopy and immunocytochemical analysis. Subsequently, MRI phantoms could be prepared and iron determination, MTT assays and FACS analysis could be performed.

2.1 Subjects and cell culture

Healthy human third molars were collected from 13 patients patients aged 15-20 years (mean=16,38; s.d.=1,38) with informed consent at the Instituut voor Mond-, Kaak- en Aangezichtsheelkunde at the Ziekenhuis Oost-Limburg, Campus St-Jan. The tooth surface was disinfected with 75% alcohol. Next, the tooth was fractured mechanically to reveal the pulp tissue which was then isolated and cut into small fragments of 1-2mm^3. These fragments were then put into explant culture using 6-well plates (Nunclon™, Roskilde, Denmark) in alpha modification of minimum essential medium supplemented with 10% fetal calf serum (FCS), 100µM L-ascorbic acid (Sigma®, St. Louis, United states of America), 2mM L-glutamine, 100U/ml penicillin, 100µg/ml streptomycin. Explants were incubated at 37°C in a humidified atmosphere containing 5% carbon dioxide (CO_2). The culture medium was changed every 3-4 days and explants were evaluated on a regular basis with a Nikon Eclipse TS100 inverted phase contrast microscope equipped with a Jenoptik Progress C3 camera (Jenoptik, Jena, Germany) with corresponding Progress Capture Pro 2.7 software. All products were obtained from Gibco®/Invitrogen™ , Paisley, United Kingdom unless stated otherwise.

BMMSCs were collected at the Ziekenhuis Salvator, Hasselt, from one patient undergoing craniofacial surgery, requiring the use of autologous BMMSC to improve the surgical outcome. Cells were cultured in Dulbecco's Modified Eagle Medium with GlutaMax™ supplemented with 100U/ml penicillin and 100µg/ml streptomycin.

After reaching 70-80% confluence, cells were harvested using 0,05% Trypsin with ethylenediaminetetraacetic acid (EDTA). Following dissociation from the cell culture plate, the cell suspension was pelleted at 300g for 5 minutes using an Eppendorf 8510 centrifuge (VWR, Leuven, Belgium). The amount of cells in suspension was counted using a 0,4% Trypan Blue Stain solution and a Fuchs Rosenthal counting chamber (Optik Labor Frischknecht, Balgach, Switzerland). For further expansion, the cells were seeded at a density

of 4 x 10^3 cells/cm^2 (25cm^2 or 75cm^2 culture flasks; Nunclon™, Roskilde, Denmark). The cell culture medium was changed every 3-4 days. Cells were used from passage numbers ranging from 1 to 7.

For basal immunocytochemical or TEM analysis, DPSCs and BMMSCs were seeded in 24 well plates (Greiner Bio-one, Wemmel, Belgium) covered with glass coverslips (Thermo-Scientific; Menzel-Gläser, Braunschweig, Germany) or Thermanox® (Nunc™, New York, United States of America) coverslips respectively at a density of 5 x 10^3 cells/cm^2 in 0,5ml of standard culture medium.

2.1.1 Neural differentiation of DPSCs

To subject DPSCs to neural differentiation, cells were seeded at a density of 5 x 10^3 cells/cm^2 on Hydrocell™ 24 multi dish plates (Nunc™, Roskilde, Denmark) in DMEM with Ham's nutrient mixture F12 (DMEM/F12) supplemented with 2% B27, 100U/ml penicillin, 100µg/ml streptomycin, 20ng/ml EGF and 20ng/ml bFGF (both purchased from ImmunoTools, Friesoyhte, Germany). The cells were incubated at 37°C in a humidified atmosphere containing 5% CO_2. The differentiation medium was changed every 2-3 days and neurospheres were harvested after 7-9 days. Mature neurospheres were then transferred to Poly-L-Ornithine (15µg/ml; Sigma-Aldrich, Bornem, Belgium) and fibronectin (4µg/ml; R&D systems, Minneapolis, MN, United States of America) coated glass- or Thermanox® coverslips in a standard 24 well plate. Neurospheres attached to this coated surface allowing the cells to migrate out of the neurospheres, forming a monolayer. Differentiation medium was again changed every 2-3 days. After 14 days, the cells were fixated for ICC or TEM analysis.

2.1.2 Labelling DPSCs with Endorem® and Poly-L-Lysine

The seeding density of DPSCs prior to labelling them with Endorem® and PLL varied between various experiments and will therefore be mentioned in the corresponding sections. A working solution of 5mg/ml Endorem® (Guerbet, Villepinte, France) was prepared out of an 11,6 mg/ml stock solution while a working solution of 30µg/ml PLL (Sigma®, St. Louis, United states of America) was used. DPSC samples were collected from cells in passage numbers ranging from 1 to 9. To demonstrate cellular iron content cytochemically, Perls' iron staining was performed (see supplemental material and methods).

Labelling conditions for each experiment consist of 0µg/ml PLL + 0µg/ml Endorem®; 0µg/ml PLL + 15µg/ml Endorem®; 0µg/ml PLL + 25µg/ml Endorem®; 0µg/ml PLL + 50µg/ml Endorem®; 0,75µg/ml PLL + 0µg/ml Endorem®; 0,75µg/ml PLL + 15µg/ml Endorem®; 0,75µg/ml PLL + 25µg/ml Endorem®; 0,75µg/ml PLL + 50µg/ml Endorem®; 1,5µg/ml PLL + 0µg/ml Endorem®; 1,5µg/ml PLL + 15µg/ml Endorem®; 1,5µg/ml PLL + 25µg/ml Endorem®; 1,5µg/ml PLL + 50µg/ml Endorem®.

The influence of PLL-Endorem® labelling on neurogenic differentiation of DPSCs was evaluated with the experimental determined optimal labelling concentration in a pilot experiment (n=2). After labelling DPSCs with the optimal PLL-Endorem® concentration, the labelled cells were subjected to neural differentiation as described above.

2.2 Immunocytochemistry

Cells adhered to glass coverslips are fixated in Unifix, a fixative containing formaldehyde (Klinipath, Duiven, The Netherlands), for 20 minutes prior to preparation. The peroxidase-based EnVision System® (Dakocytomation, Glostrup, Denmark) was used to perform immunocytochemical stainings. After fixation, the samples were rinsed three times in 0,01M phosphate buffered saline (PBS; pH=7,2). Whether the target epitope of the primary antibody was located intra- or extracellularly, the samples were permeabilized with 0,05% Triton X-100 (Boehringer, Mannheim, Germany) in PBS for 30 minutes at 4°C. After permeabilization, the samples were washed four times with PBS before blocking aspecific binding sites with 3% normal goat serum (NGS; Dakocytomation, Glostrup, Denmark) in PBS for 20 minutes. The samples were washed four times with PBS before adding the primary antibodies. Primary antibodies were incubated for one hour (Table 1).

Table 1: overview of the primary antibodies used for immunocytochemical analysis. RP= Rabbit Polyclonal; MM= Mouse Monoclonal; RTU= Ready To Use

Primary antibody	Species	Dilution	Source (clone)
CD146	RP, IgG_1	RTU	Abcam®
S100	RP	1/400	DakoCytomation
Glial Fibrillary Acid Protein (GFAP)	MM, IgG_1	1/100	Novocastra Laboratories (GA5)
Neuronal Neuclei (NeuN)	MM, IgG_1	1/100	Millipore (A60)
Ki67	MM, IgG_1	1/75	Immunosource (MIB-1)
A2B5	MM, IgM	1/200	Chemicon® International (105)
Galactosylceramidase (GalC)	MM	1/10	Dr.Yong, Calgary Univ (H8H9)
Protein Gene Product 9.5 (PGP9.5)	MM, IgG2b	1/500	Novocastra Laboratories(10A1)
CD34	MM, IgG1	1/50	Abcam® (BI-3C5)
Nerve Growth Factor Receptor p75 (NGFRp75)	MM, IgG_1	1/150	Abcam® (ME20.4)
CD44	MM, IgG_1	1/200	Abcam® (NKI-P2)
CD105	MM, IgG_1	1/1000	Abcam® (105C02)
CD29	MM, IgG_1	1/50	Abcam® (4B7R)
STRO-1	MM, IgM,	1/50	R&D systems
Neurofilament protein (NF)	MM, IgG_1	RTU	DakoCytomation (2F11)
Synaptophysin	MM, IgG_1,	1/20	DakoCytomation (SY38)
Vimentine	MM, IgG_1	1/50	DakoCytomation (V9)
Beta-Tubulin III (Neuronal)	MM, IgG2a	1/2000	Sigma-Aldrich® (2G10)
Nestin	MM, IgG1	1/500	Millipore (10C2)
Neuron Specific Enolase (NSE)	RP	RTU	Dako Corporation
Neural Cell Adhesion Molecule (NCAM)	MM, IgG1	1/250	Novocastra Laboratories (1B6)

Prior to adding the secondary antibody, the samples were washed four times with PBS. Horseradish peroxidase-conjugated goat anti-mouse/rabbit secondary antibodies from the EnVision kit were used, depending on the primary antibody. After labelling the samples with the secondary antibody for 30 minutes at room temperature, they were washed four times with PBS and stained by the 3,3' diaminobenzidine chromogen solution of the EnVision kit. Afterwards, the Mayer's hematoxylin nuclear counterstain was performed. The samples were mounted with Aquatex® (Merck, Darmstadt, Germany) on glass slides (Thermo-Scientific; Menzel-Gläser, Braunschweig, Germany). Samples were evaluated using a Nikon Eclipse 80i (Nikon, Japan) light microscope with complementary digital camera. Digital images were processed using corresponding LNET software.

2.3 Transmission electron microscopy

Samples grown on plastic Thermanox® coverslips were fixated with 2% glutaraldehyde (Laborimpex, Brussels, Belgium) in 0,05M sodium cacodylate buffer (Aurion, Wageningen, The Netherlands) (pH=7,3) at 4°C. Afterwards, the samples were washed twice for 5 minutes with 0,05M sodium cacodylate (pH=7,3) and 0,15M saccharose at 4°C. Postfixation was achieved by treating the samples with 2% osmiumtetroxide (Aurion, Wageningen, The Netherlands) in 0,05M sodium cacodylate buffer (pH=7,3) for 1 hour at 4°C. Dehydration of the samples was performed by exposing them to ascending concentrations of aceton. The dehydrated sample was impregnated overnight in a 1:1 mixture of aceton and araldite epoxy resin (Aurion, Wageningen, The Netherlands) at room temperature. After impregnation, the sample was embedded in araldite epoxy resin at 60°C using the pop-off method. The embedded samples were cut in slices of 40-60nm, making use of a Leica EM UC6 microtome (Leica, Groot Bijgaarden, Belgium). Slices were then transferred to 50 mesh copper grids (Aurion, Wageningen, The Netherlands) coated with 0,7% formvar. The samples were contrasted using a Leica EM AC20 (Leica, Groot Bijgaarden, Belgium) with 0,5% uranyl acetate and a stabilized solution of lead citrate (both from Laurylab, Saint Fons, France). TEM analysis was performed with a Philips EM208 S electron microscope (Philips, Eindhoven, The Netherlands). The microscope was provided with a Morada Soft Imaging System camera to acquire high resolution images of the evaluated samples. The images were processed digitally with iTEM-FEI software (Olympus SIS, Münster, Germany).

2.4 Magnetic Resonance Imaging of Poly-L-Lysine/ Endorem® labelled DPSCs

DPSCs were seeded at a density of 10 x 10^3 cells/cm^2 in a 24 well plate. After incubating the seeded cells for 24h (37°C; 5% CO2 in humidified air) the cells were labelled with the appropriate labelling conditions. When the cells were exposed to the labeling condition for 24h, the labeling solution was removed and the cells were rinsed with PBS to remove any remaining iron particles. Cells were then either kept in culture for two more days in standard culture medium or were immediately processed to create MRI phantoms (24h labelling n=4; 3d labelling, n=2) in order to evaluate the visualization of labelled DPSCs with MRI.

To create MRI phantoms, the cells were trypsinized, pelleted at 300g and resuspended in standard culture medium. Due to the high interpersonal variation in determining cell numbers using standard counting procedures, cell numbers were based on the control samples. Moreover, the absolute cell numbers were not considered significantly different both

between- and within different labelling conditions. After counting, the cells were pelleted at 300g and resuspended in PBS. Using a 1:1 ratio of 200µl PBS containing 500 cells/µl and 200µl of 0,5% agar in distilled water (Sigma Aldrich, St Louis, USA), a cell suspension of 250 cells/µl was transferred to an eppendorf tube 1/3 prefilled with solidified agar. After hardening of the PBS/agar mixture, the eppendorf tube was filled entirely with agar. After solidification, The different eppendorfs were placed in a purpose-built Teflon holder and placed in a plastic cup. Subsequently the holder was completely immersed in agar and capped. The completed phantoms were analyzed with a Bruker Biospec 9.4 Tesla small animal MR scanner (Bruker Biospin, Ettlingen, Germany; horizontal bore, 20cm) equipped with actively shielded gradients (600mT m^{-1}) at the Catholic University of Leuven. These scans led to 3D-high resolution T2* weighted MRI images, enhanced T2 weighted images, from which the relative signal intensity of the analyzed samples could be obtained.

2.5 MTT cell viability assay of Poly-L-Lysine/Endorem® labelled DPSCs

Cells from each sample were seeded at a density of 15 x 10^3 cells/cm^2 in a 96 well plate (Nunc™, Roskilde, Denmark). After incubating the seeded cells for 24 h (37°C; 5% CO2 in humidified air) the cells were labelled with the appropriate PLL/Endorem® condition. Each labelling condition was made in triplet in all individual samples (n=10). When the cells were exposed to the labelling condition for 24h, the labelling solution was removed and cells were rinsed with PBS before normal culture medium was added to remove any remaining iron particles. Cells were then kept in culture for two more days, after which the 3-(4,5-dimethylthiazol-2-Yl)-2,5- diphenyltetrazolium bromide (MTT) assay was performed in order to evaluate cell viability/metabolic activity after three days of exposure to the Endorem® particles. Culture medium containing 10% dimethylsulfoxide (DMSO; Sigma-Aldrich Chemie, Steinheim, Germany) was used to induce cell death serving as a control for the MTT test.

In order to analyze the cells, the medium was removed and replaced with a solution containing 5% MTT (working solution: 5mg/ml; Sigma-Aldrich, Bornem, Belgium), after which the cells were incubated for 4h (37°C; 5% CO_2 in humidified air). Secondly, the MTT solution was removed and replaced with 175µl of a mixture containing 14% Glycine (0,1M; Sigma Aldrich, St Louis, USA) in DMSO. This solution dissolved the purple crystals (a formazan) that were formed out of yellow MTT (a tetrazol) in the mitochondria of living cells making it possible to measure the absorbance of the solution at 540nm with an iMark™

Microplate Reader (BIO-RAD, Nazareth, Belgium). The amount of absorbance was a measurement of cell viability or metabolically active cells, as only viable cells are able to catalyze the conversion of yellow MTT to the purple formazan.

2.6 Determination of cellular iron uptake after Poly-L-Lysine/Endorem® cell labelling

Cells from each sample (n=3) were seeded at a density of 50 x 10^3 cells/cm^2 in a 6 well plate. After 24 hours, the cells were subjected to the appropriate labelling PLL/Endorem® conditions as stated above. One day after incubating the cells with the loading medium, this medium was removed and the cells were subsequently cultured under standard culture conditions for two more days. Afterwards, the cells were trypsinized, pelleted at 300g and resuspended in nitric acid to dissolve the cells and free all iron content.

The iron concentration was determined by AAS using a Perkin-Elmer 1100B atomic absorption spectrophotometer (PerkinElmer, Waltham, Massachusetts, USA). The sample was firstly vaporized and subsequently atomized with an acetylene-oxygen driven flame. A Fe-selective hollow cathode emitting light at 248,3 nm was used as an excitation source for the iron particles in the sample. The atomized sample absorbs energy at this specific wavelength and as the amount of emitted energy was known, the absorbance of the emitted light was a measurement for the iron content in the sample.

2.7 Fluorescence activated cell sorting

The fraction of DPSCs positive for STRO-1 or NGFRp75 was determined using a Becton-Dickinson FACSCalibur™ (BD Biosciences, Erembodegem, Belgium). Primary antibodies for both markers were used as described in Table 1, with a dilution of 1/100 and 1/50 for NGFRp75 and Stro-1 respectively. Simultest ™ IgG1-FITC/IgG2a-PE (BD, San Jose, California, United States of America) was used as an IgG_1 isotype control for NGFRp75, while a mouse IgM isotype control (clone 11E10; eBiosciences, San Diego, California, United States of America) was used for Stro-1. Dilutions were made according to the primary antibody. A Fluorescein Isothiocyanate (FITC) labelled goat anti mouse isotype (Molecular Probes, Invitrogen ™; Paisley, United Kingdom) secondary antibody was used in a dilution of 1/300. Samples (n=3) were analyzed with Cellquest Software (BD Biosciences, Erembodegem, Belgium).

2.8 Statistical analysis

Statistical analysis was performed using Graphpad Prism 5 software (Graphpad, California, USA). Significant differences between experimental groups were determined using the one way analysis of variance (ANOVA) test with a Bonferroni or Tukey post test after controlling for normality with a D'Agostino and Pearson test or normalizing the data. Data were represented as mean ± standard error of the mean (S.E.M.). P-values $\leq 0,05$ were considered statistically significant at the 5% significance level.

3 Results

In this section the morphological and immunophenotypical analysis of differentiated and undifferentiated DPSCs are listed. In addition to the analysis of general MSC markers, the presence of neural markers is evaluated in differentiated and undifferentiated DPSCs. The basal expression of neural markers in DPSCs and BMMSCs is compared. Ultrastructural analysis of differentiated DPSCs is also presented.

A second part of the present study comprised the labelling of DPSCs with Endorem® particles. Firstly, the cells were visualized with MRI both one day and three days after labelling. Next, the labelling conditions considered most suitable based on the MRI experiments were analyzed using TEM three days post labelling. The intracellular distribution of the Endorem® particles was assessed in addition to an evaluation of cell morphology. Based on these results, cellular viability/metabolic activity and cellular iron content after labelling were determined with a MTT- and AAS assay respectively to assess whether the chosen ratios led to a preservation of cell viability and whether a significant increase in cellular iron content was present.

3.1 Morphological features of DPSCs

Morphological features of DPSCs are represented in Figure 1. Pulp explants attach to the plastic culture dishes after one week in culture, leading to an outgrowth of adherent DPSCs (Figure 1A). DPSCs show a heterogeneous morphological appearance with cell shapes ranging from small, spindle-like cells to fan-shaped cells *in vitro* (Figure 1B). Morphological features of BMMSCs are presented in supplemental data, Figure S1.

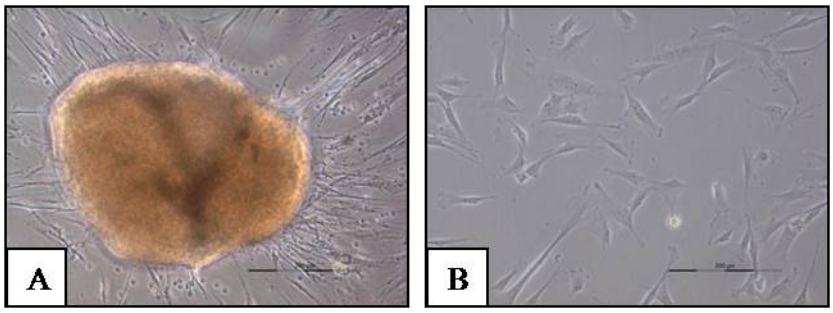

Figure 1: Morphological characteristics of pulp explants (A) and DPSCs in cell culture (B). DPSCs are constituted of a heterogeneous cell population with a variety of cell shapes ranging from spindle- to fan-shaped cells with irregularly distributed cell extensions. (scale bars= 200µm).

3.2 Immunocytochemical analysis of DPSCs

Immunocytochemical stainings were performed to ensure MSC properties of DPSCs. The presence or absence of general MSC markers is evaluated. These data are presented in Figure 2. DPSCs are positive for the MSC markers CD29, CD44, CD105, CD146 (Figure 2 A-D), show immunoreactivity for CD117 (Figure 2E) in a subset of cells and are negative for CD34 (Figure 2F). DPSCs are positive for the mesenchymal cell marker vimentin (Figure 2G) and the NSC/neural precursor cell marker nestin (Figure 2I). Immunoreactivity for the suggested marker for more potent MSCs, Stro-1, is found to be present in 5,8% of the cells (n = 8; s.d 2,2%) (Figure 2H). Immunoreactivity of BMMSCs for the identical markers is represented in Supplemental data Figure S2.

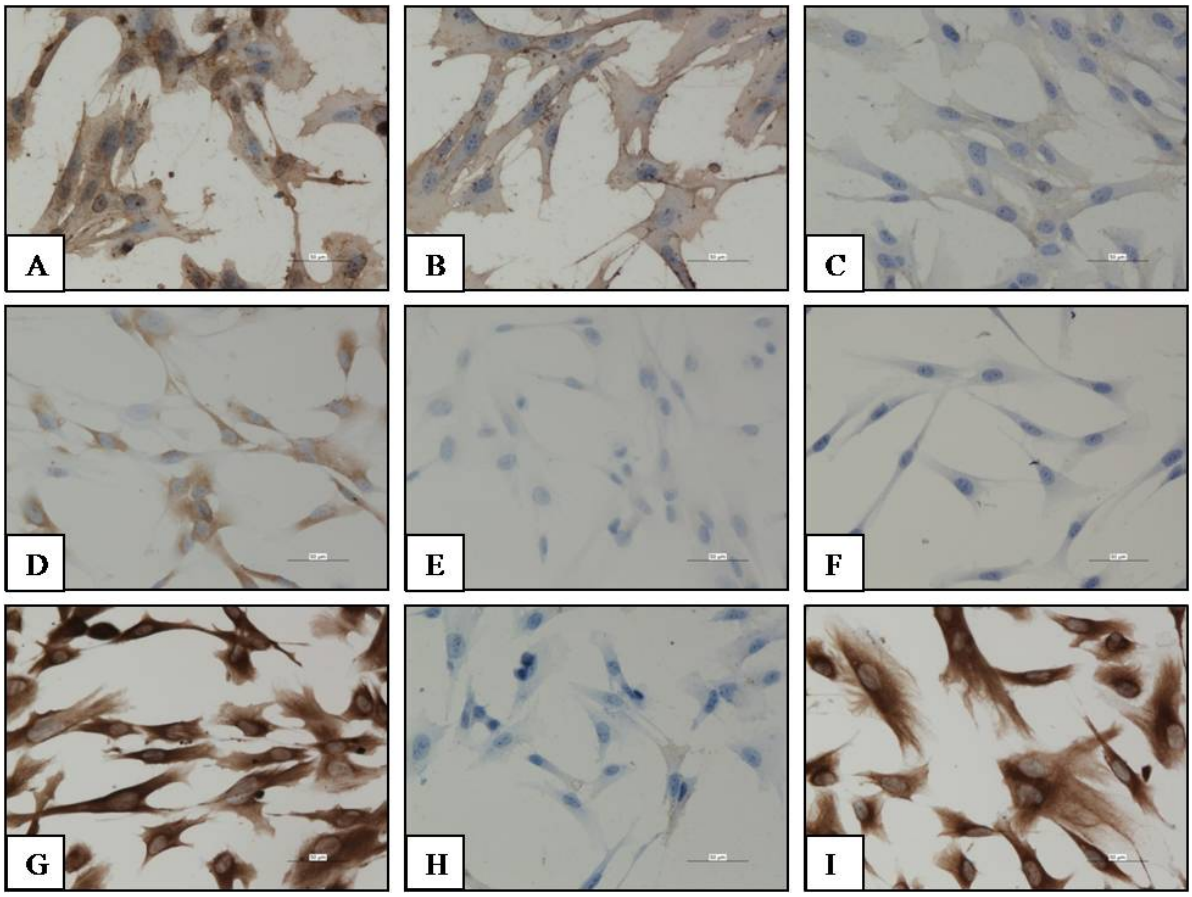

Figure 2: Immunophenotype of DPSCs. DPSCs show immunoreactivity for the MSC markers CD29 (A); CD44 (B), CD105 (C); CD146 (D). Immunoreactivity for CD117 (E) is observed in a subset of DPSCs. DPSCs are negative for CD34(F) and are positive for vimentin (G) and nestin (I); The presence of the suggested marker for more potent MSCs, Stro-1, was found in 5,8% of the cells (H, n=8; s.d.= 2,2%). (scale bars= 50µm)

3.2 FACS analysis of DPSCs for NGFRp75 and Stro-1

Using FACS analysis, the percentage of DPSCs positive for NGFRp75 or Stro-1 was determined (Figure 3). The reported values are calculated by subtracting the background signal for the secondary antibody from the percentage of positive cells in each experimental group. This leads to an average fraction of 2,11% (n=3; s.d. = 1,45%) and 6,92% (n= 3; s.d. = 4,26%) positive DPSCs for NGFRp75 (Figure 3A) and Stro-1 (Figure 3B) respectively.

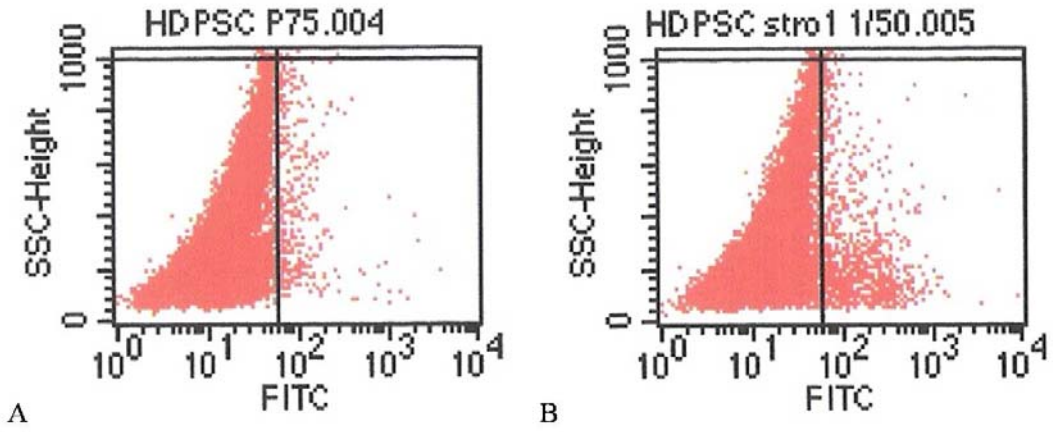

Figure 3: FACS analysis shows a fraction of 2,11% (n=3; s.d. = 1,45%) and 6,92% (n= 3; s.d. = 4,26%) positive DPSCs for NGFRp75 (A) and Stro-1 (B) respectively.

3.3 Neurogenic differentiation of DPSCs

In this next section, neural differentiation of DPSCs using bFGF and EGF as inducing agents is evaluated. Morphological changes of DPSCs and alterations in immunophenotypical profile for neurogenic markers are discussed. In addition, the ultrastructural appearance of differentiated DPSCs is presented.

3.3.1 Morphological features of neurogenic differentiated DPSCs

Inducing neurogenic differentiation with bFGF and EGF on low-attachment cell culture plates leads to the formation of free floating neurospheres (Figure 4A). Seven days after incubation, the neurospheres were transferred to Poly-L-Ornithine and fibronectin coated cell culture plates. This allowed outgrowth of differentiated DPSCs out of neurospheres (Figure 4B). Differentiated DPSCs show a bipolar morphology with an apparent elongation of cellular processes (Figure 4C).

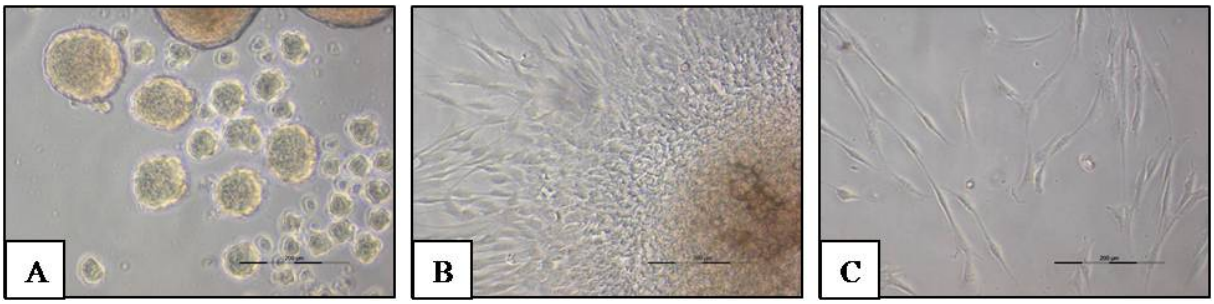

Figure 4: Neurogenic induction of DPSCs leads to neurosphere formation (A) that allows cellular outgrowth when transferred to Poly-L-Ornithine and fibronectin coated cell culture plates (B). After neurosphere outgrowth, DPSCs show a bipolar morphology with an apparent elongation of cellular processes (C). (scale bars= 200µm)

3.3.2 Ultrastructural evaluation of neurogenic differentiated DPSCs

Ultrastructural evaluation of both undifferentiated and differentiated DPSCs is presented in Figure 5. Undifferentiated DPSCs show a heterogeneous cell morphology with a perinuclear distribution of cell organelles (Figure 5A). Furthermore, an electron-lucent, organelle-free peripheral border is observed. Compared with undifferentiated cells, the differentiated cells show long cytoplasmatic extensions and prominent, uniformly distributed cell organelles (Figure 5B). Although undifferentiated cells show a prominent Golgi apparatus and vesicular activity (Figure 5C), these seem more pronounced in differentiated cells (Figure 5D). Both undifferentiated and differentiated cells are able to form cell-cell junctions (Figure 5 E and F respectively; black arrows)

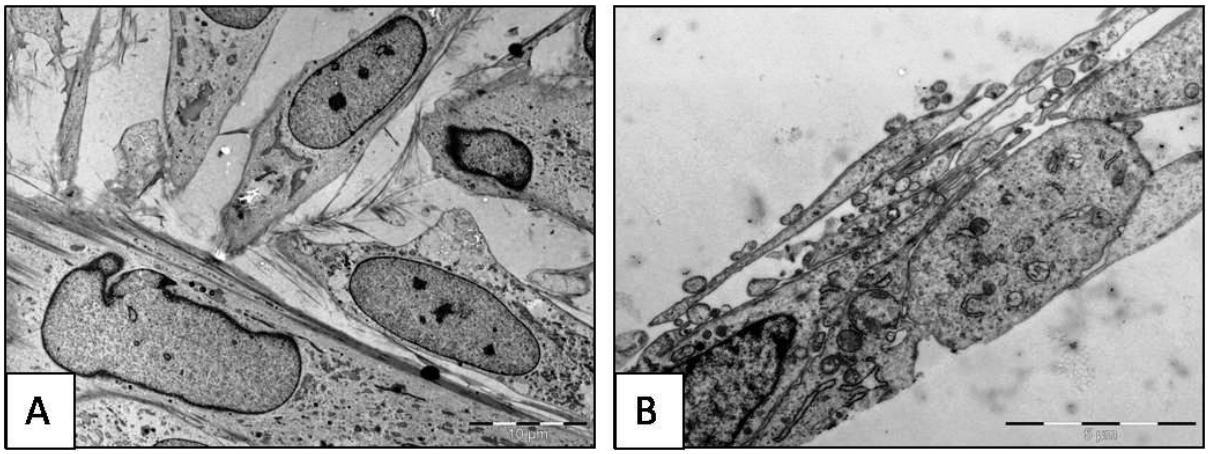

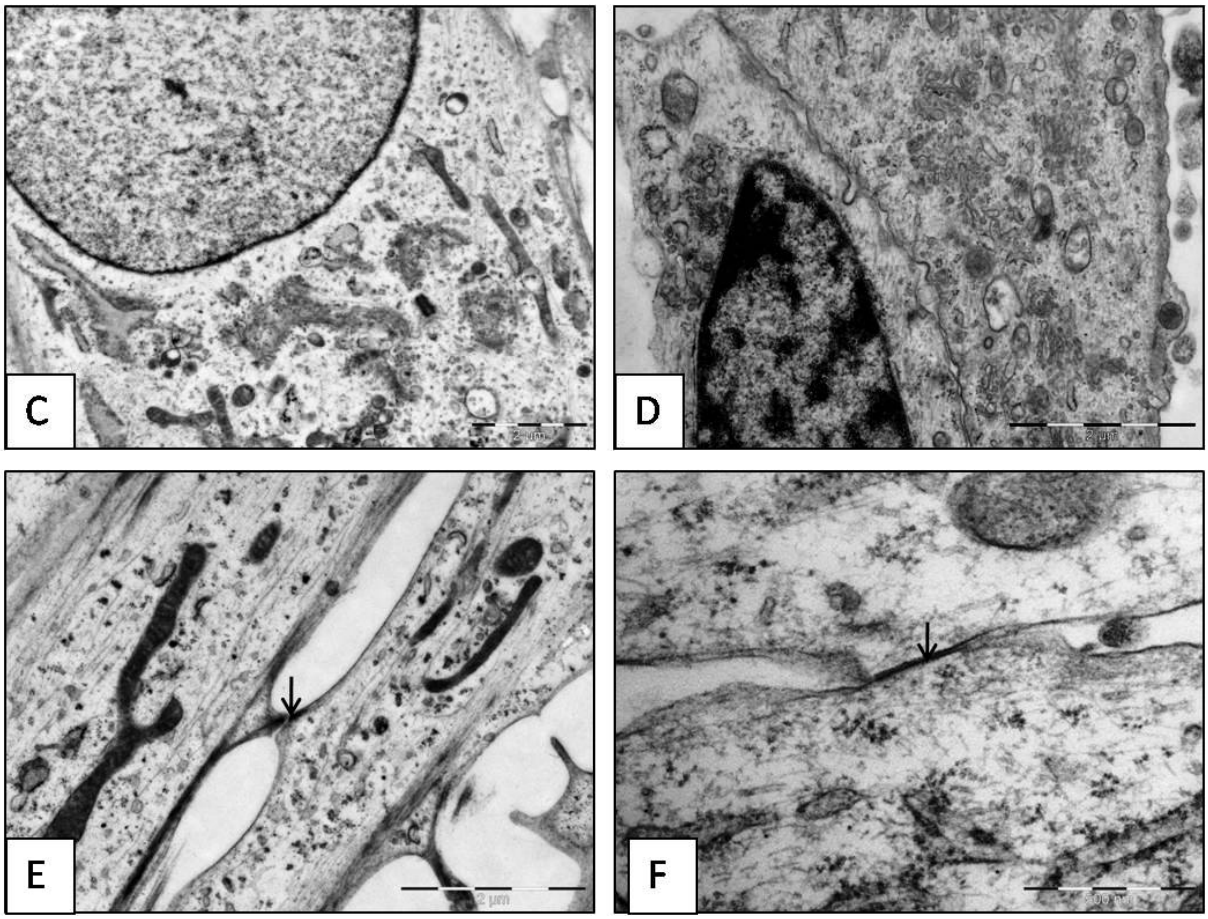

Figure 5: ultrastructural evaluation of neurogenic differentiated DPSCs compared to undifferentiated DPSCs. Undifferentiated DPSCs show a heterogeneous cell morphology (A) while differentiated DPSCs show long cytoplasmatic extensions (B). A perinuclear distribution of cellular organelles is observed in undifferentiated DPSCs (A, C). Differentiated cells show prominent, uniformly distributed cell organelles (B, D). Undifferentiated cells show a prominent Golgi apparatus and vesicular activity (B) but these are more pronounced in differentiated DPSCs (D). Both undifferentiated and differentiated cells are able to form cell-cell junctions (E and F respectively; black arrows). (scale bars: A = 10µm; B, D, E= 2µm; C= 5µm; F= 500nm)

More detailed images of neurogenic differentiated DPSCs are presented in Figure 6. These images show the presence of electron dense vesicles at cell-cell contact zones with a diameter varying from 35-50nm (Figure 6A; black arrows). In addition, the release of vesicles is observed at cell-cell contact zones. (Figure 6B)

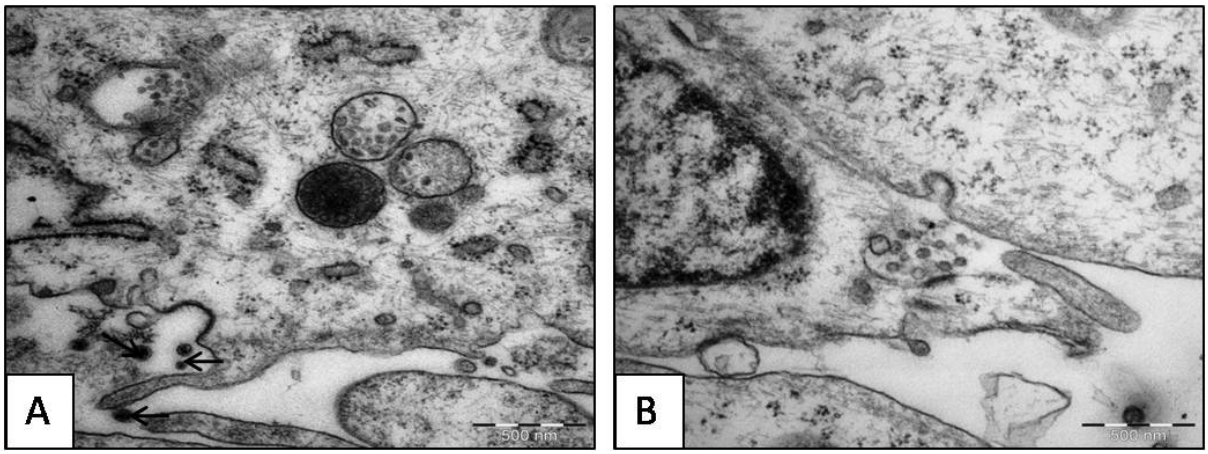

Figure 6: detailed images of differentiated DPSCs show electron dense vesicles at cell-cell contact zones (A; black arrows). The release of vesicles between cells is observed (B). (scale bars: A, B = 500nm)

3.3.3 Immunocytochemical analysis of neurogenic differentiated DPSCs

Neurogenic differentiated (n≥1) and undifferentiated (n=3) DPSCs were subjected to immunocytochemical analysis for the neural markers beta-III tubulin, neurofilament, S-100, synaptophysin, NSE, GalC, A2B5, GFAP, PGP9.5, NCAM, NGFRp75 and NeuN. The results of this analysis can be found in Figure 7 A-L and Figure 8 A-L for undifferentiated and differentiated DPSCs respectively. The basal expression for the suggested markers in BMMSCs is presented in supplemental data Figure S3.

Undifferentiated cells showed immunoreactivity against beta III tubulin, S-100, synaptophysin, NSE, GalC, A2B5 and NGFRp75 (Figure 7 A, C-G). Expression for neurofilament and NGFRp75 was observed in a subset of cells (Figure 7 B and K respectively). Expression of GFAP, PGP9.5, NCAM and NeuN could not be detected (Figure 7 H-J, L)

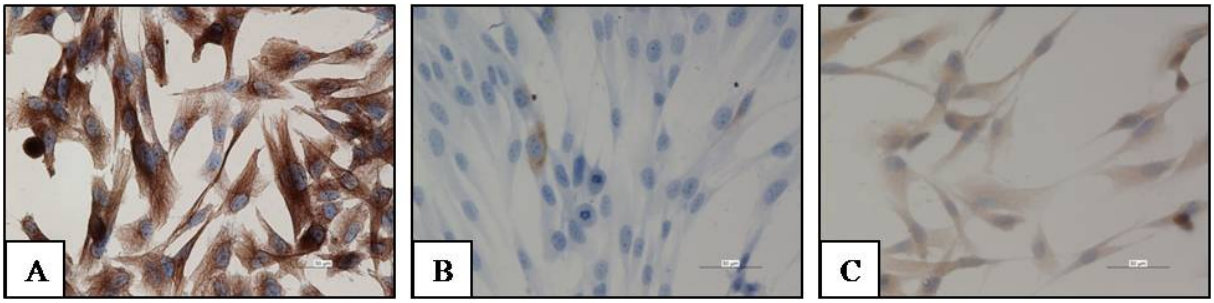

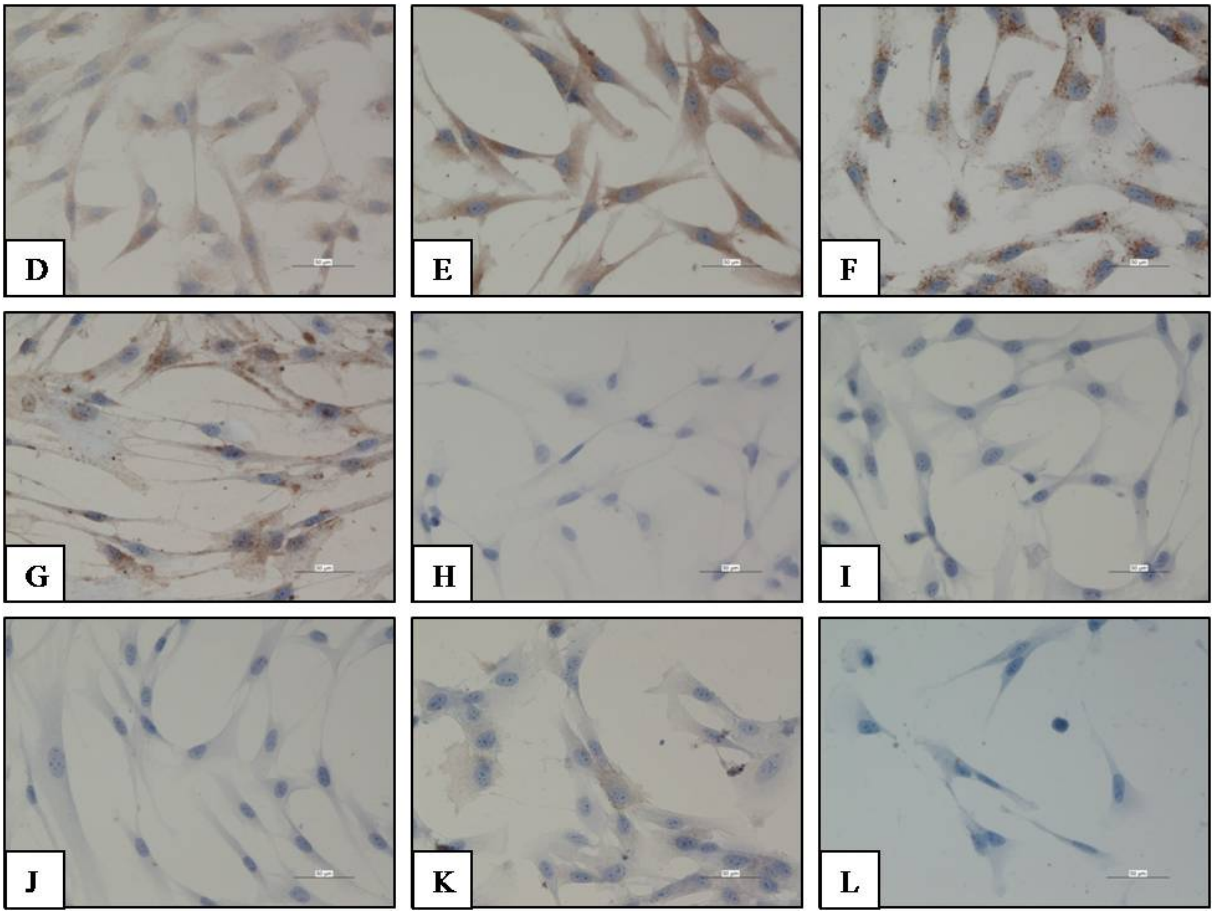

Figure 7: Basal immunoreactivity of DPSCs to beta-III tubulin, neurofilament, S-100, synaptophysin, NSE, GalC, A2B5, GFAP, PGP9.5, NCAM, NGFRp75 and NeuN (A-L respectively). Immunoreactivity was observed in beta III tubulin, S-100, synaptophysin, NSE, GalC and A2B5 but not in GFAP, PGP9.5, NCAM and NeuN. Expression of neurofilament and NGFRp75 was observed in a subset of cells. (scale bars= 50µm)

Following differentiation, DPSCs showed immunoreactivity against beta III tubulin, S-100, synaptophysin, NSE, GalC, A2B5 and NeuN (Figure 8 A, C-G, L). Neurofilament and NGFRp75 were expressed in a subset of differentiated cells (Figure 8 B and K respectively). Expression of GFAP, PGP9.5, NCAM could not be detected (Figure 8 H-J). NGFRp75 positive cells in the undifferentiated cell group only show slight immunoreactivity as compared with the differentiated cells, which show an increased response both in apparent numbers and immunoreactivity. The only marker for which a clear distinction between differentiated and undifferentiated could be made was NeuN. Undifferentiated cells were negative for NeuN, while differentiated cells showed responsiveness in a large fraction of the analyzed cells.

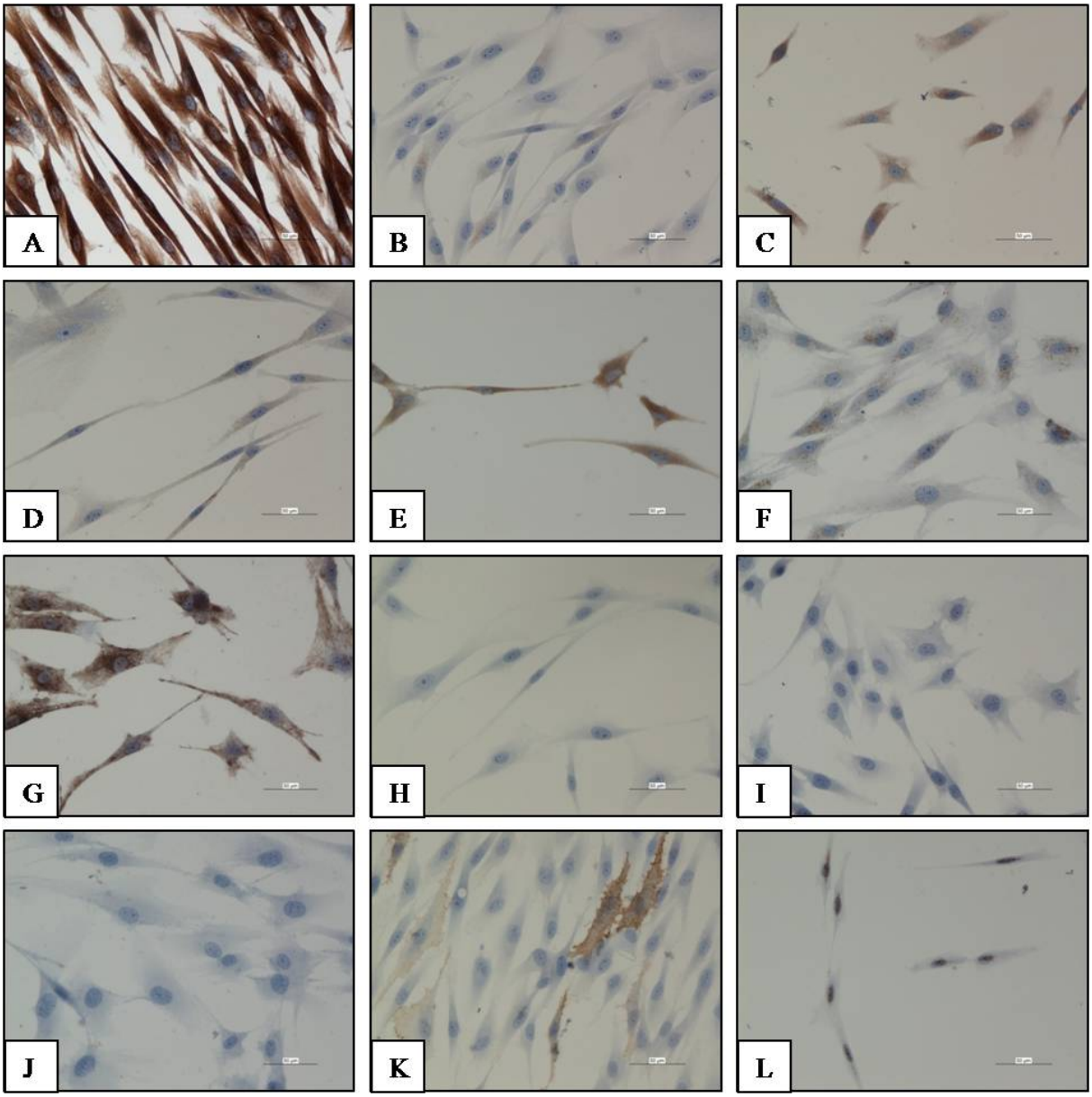

Figure 8: immunocytochemical analysis of neural associated markers in differentiated DPSCs. Markers include beta-III tubulin, neurofilament, S-100, synaptophysin, NSE, GalC, A2B5, GFAP, PGP9.5, NCAM, NGFRp75 and NeuN (A-L respectively). Immunoreactivity was observed in beta III tubulin, neurofilament, S-100, synaptophysin, NGFRp75, NSE, GalC, A2B5 and NeuN but not in GFAP, PGP9.5 and NCAM. NGFRp75 seems to be upregulated following neurogenic differentiation. (scale bars= 50µm)

3.5 MRI analysis of Poly-L-Lysine/Endorem® labelled DPSCs

In this section the ability of labelled DPSCs to be visualized with MRI is discussed. Scans were taken 24 hours and three days post-labelling. MRI scans were taken of the constructed phantoms to evaluate the cellular contrast due to iron oxide particle uptake both 24 hours (n=4) and three days (n=2) after labelling DPSCs with PLL and Endorem® (Figure 9a and 9b respectively). MRI images of both conditions show that in the absence of PLL there is a

gradual increase in contrast as the Endorem® concentration rises from 0µg/ml to 50µg/ml (Figure 9a and 9b; A-D). However, the addition of 0,75µg/ml PLL combined with 15µg/ml Endorem® leads to a drastic increase in contrast (Figure 9a and 9b; F). Increasing both the PLL as the Endorem® concentration does not lead to a further increase in contrast. Labelling conditions that do not include Endorem® particles do not show an increase in contrast (Figure 9a and 9b; A, E, I).

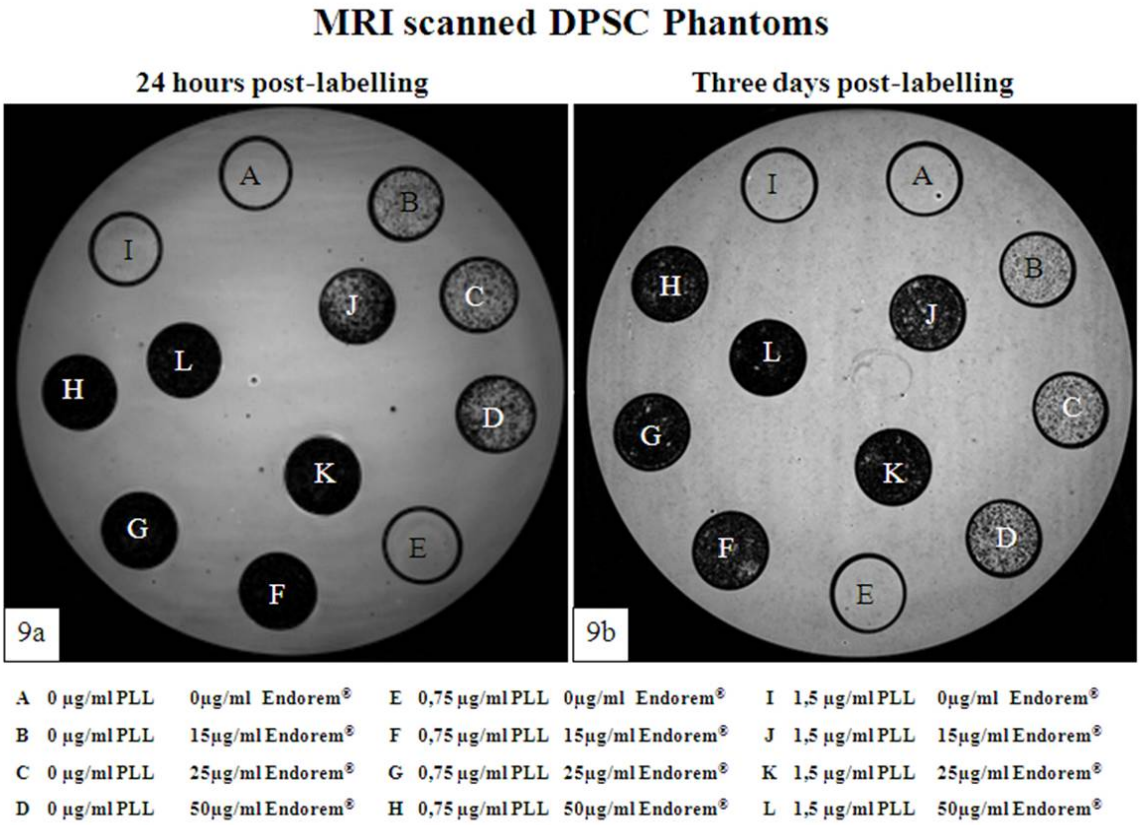

Figure 9: MRI images of DPSCs 24 hours (9a) and three days after (9b) cell labelling. Both time points are characterized by comparable outcomes. The addition of PLL does not alter cellular MRI contrast (E, I) compared to the control condition (A). A stepwise increase of the iron content from 0µg/ml to 50µg/ml Endorem® without the addition of PLL gradually increases the observed contrast (B-D). However, the addition of 0,75µg/ml PLL to 15µg/ml Endorem® (F) leads to a drastic increase in cellular contrast in MRI. Further increments in iron content or PLL do not lead to a higher observed contrast (G, H, J, K, L).

These results can be translated to relative signal intensity in T2 weighted images (Figure 10). Data were normalized by defining the control condition of 0µg/ml PLL – 0µg/ml Endorem® as 100% relative signal intenisty The left panel of Figure 10 represents relative signal intensities 24 hours after labelling. All relative intensities are compared to the 0µg/ml PLL – 0µg/ml Endorem® controls. A significant decline in relative signal intensity is accompanied with an increase in contrast coupled to an augmentation in Endorem® concentration in PLL

free conditions. However, adding PLL to Endorem®, leads to an additional significant decrease in relative signal intensity. This is demonstrated by comparing the 0,75µg/ml PLL-15µg/ml Endorem® condition to the PLL-free Endorem® conditions. Significant differences between relative signal intensity are not observed between the 0,75µg/ml PLL – 15µg/ml Endorem® condition and other labelling conditions consisting of either 25µg/ml or 50µg/ml Endorem® with 0,75µg/ml PLL or 15µg/ml, 25µg/ml or 50µg/ml Endorem® and 1,5µg/ml PLL. Data were analyzed with a one way ANOVA test and a Bonferroni post test. Data are represented as S.E.M. P-values ≤ 0,05 are considered significant. The right panel of Figure 10 represents relative signal intensities three days after labelling. Analyzing the relative signal intensities three days post labelling leads to the same conclusions that 24 hours post-labelling. Coupling back these data to the MRI scans of the DPSCs phantoms shows a relationship between the increments in contrast and the decline in relative signal intensities. A further increase in contrast due to the addition of PLL to Endorem® labelling contrast in MRI scans is linked to a significant decrease in relative signal intensity between the 0,75µg/ml PLL-15µg/ml Endorem® condition compared to the PLL-free Endorem® conditions.

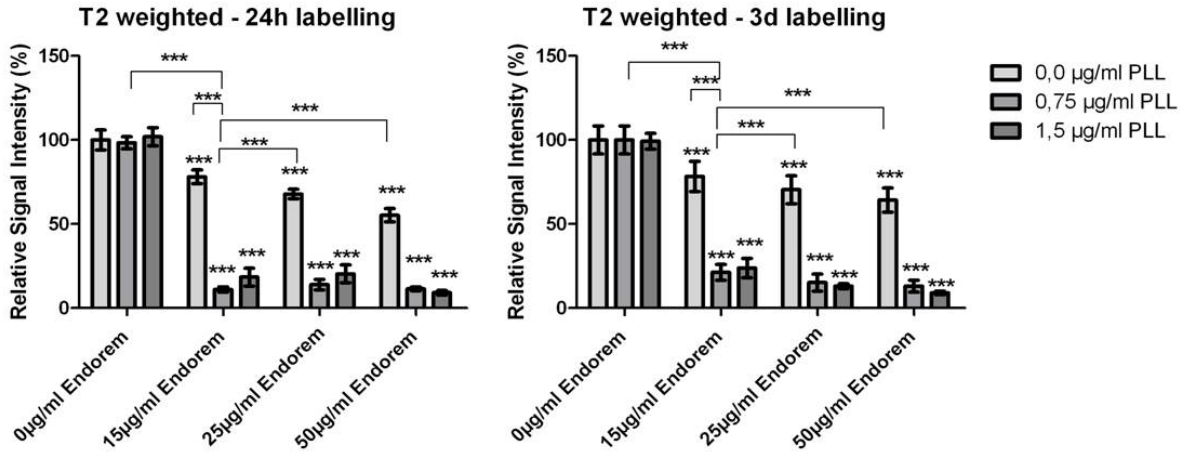

Figure 10: Relative signal intensity 24hours (left panel) and three days (right panel) after PLL/Endorem® labelling of DPSCs in T2 weighted images. Twenty-four hours after labelling, a significant decline in relative signal intensity is coupled to an augmentation in Endorem® concentration in PLL free conditions (0-50µg/ml Endorem®). Combining 0,75µg/ml PLL and 15µg/ml Endorem® leads to a significant decrease in relative signal intensity compared to the PLL-free Endorem® labelling conditions. Significant differences between relative signal intensities are not observed between the 0,75µg/ml PLL – 15µg/ml Endorem® condition and other labelling conditions consisting of both PLL and Endorem®. The same observations hold for the samples that were labelled for three days. Data were analyzed with a one way ANOVA test and a Bonferroni multiple comparison post-test. Data are represented as S.E.M.; *** = p-value ≤ 0,001

Since the 0,75µg/ml PLL – 15µg/ml Endorem® condition led to a lower relative signal intensity as compared to the PLL-free Endorem® conditions, this ratio of PLL and Endorem was compared both 24 hours and three days post-labelling. Furthermore, no significant difference could be observed between this labelling concentration and other labelling conditions consisting of both PLL and Endorem®. The results of this analysis are presented in Figure 11. As abovementioned, combining 0,75µg/ml PLL with 15µg/ml Endorem® led to a significant decrease in relative signal intensity as compared to controls. However, a significant difference in relative signal intensity is observed between labelled cells 24 hours and three days following cell-labelling. Data were analyzed with a one way ANOVA test followed by a Tukey post test. Data are represented as S.E.M. and p-values ≤ 0,05 were considered significant.

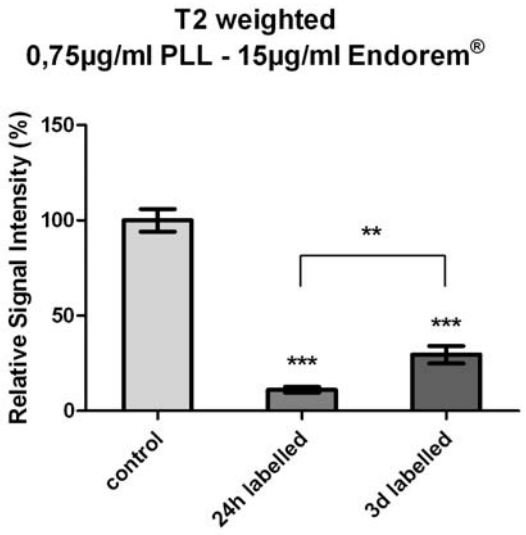

Figure 11: Relative signal intensity is compared between DPSCs labelled with 0,75µg/ml PLL and 15µg/ml Endorem® 24 hours and three days following labelling. A significant difference in relative signal intensity between both time points was observed. Data were analyzed with a one way ANOVA test followed by a Tukey post test. Data are represented as S.E.M. ** = p-value ≤ 0,01; *** = p-value ≤ 0,001

3.6 TEM analysis of Poly-L-Lysine/Endorem® labelled DPSCs

To assess the intracellular distribution and potential effects on cell morphology, TEM analysis was performed for various ratios of PLL/Endorem® considered to be most suitable for DPSC labelling based on MRI results. As the combination of 0,75µg/ml PLL and 15µg/ml Endorem® leads to a significant decrease in relative signal intensity after 24 hours and this relative signal intensity is comparable three days after DPSC labelling, these conditions were subjected to an initial TEM analysis (Figure 12). Therefore, the intracellular distribution of

these particles and potential effects on cell morphology are evaluated. The Endorem® particles do not influence cell morphology as the outer cell membrane, intracellular organelles and nucleus show no sign of abnormalities both 24 hours and three days following labelling (Figure 12 A and B respectively). Furthermore, the internalized particles are homogeneously distributed in endosomes, both 24 hours and three days post- labelling (Figure 12 A, B; black arrows). Extracellular clustering was not observed.

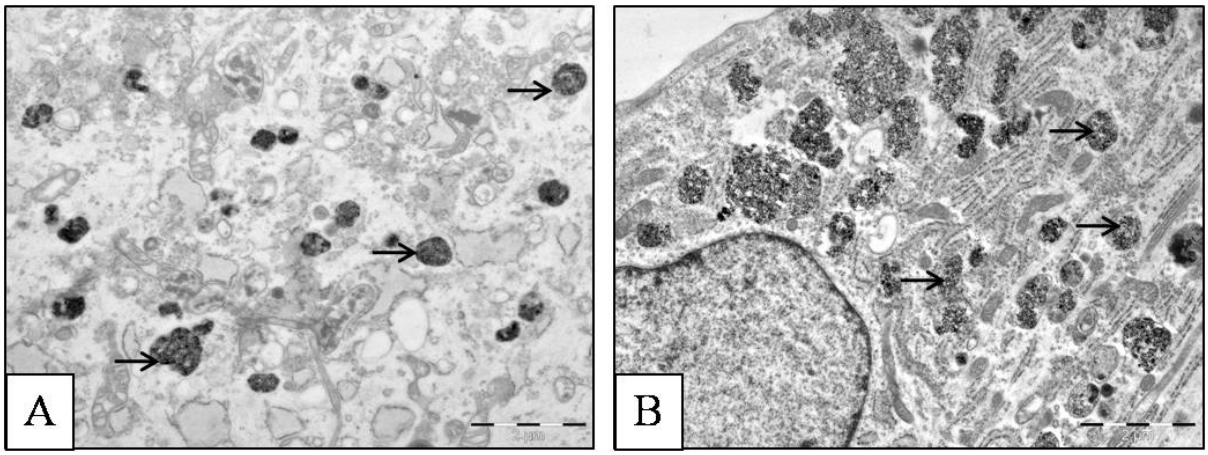

Figure 12: TEM analysis of DPSCs labelled with 0,75µg/ml PLL – 15µg/ml Endorem® 24 hours (A) and three days (B) after labelling. In both samples, cell morphology is preserved and intracellular Endorem® particles are distributed homogeneously in endosomes (black arrows). (scale bars A, B= 2µm)

As the other PLL/Endorem® ratios also influence T2 relaxation times three days post labelling, their potential effects on cell morphology and intracellular distribution are also evaluated. The ultrastructural evaluation of PLL-free Endorem® labelling conditions are left out of consideration as their influence on T2 relaxation times did not improve contrast in MRI images. An overview of the ultrastructural analysis of DPSCs three days after labelling is presented in Figure 13. Labelled samples are compared to 0µg/ml PLL – 0µg/ml Endorem® controls (Figure 13A) and include 25µg/ml or 50µg/ml Endorem®, combined with 0,75µg/ml PLL (Figure 13 B–C) or 15µg/ml, 25µg/ml and 50µg/ml Endorem® with 1,5µg/ml PLL (Figure 13 D-F).

The addition of Endorem® with either 0,75µg/ml PLL or 1,5µg/ml PLL does not alter cell morphology as the outer cell membrane, intracellular organelles and nucleus show no signs of abnormalities compared to controls. Increasing Endorem® concentrations from 15µg/ml to 25-50µg/ml in the 0,75µg/ml PLL conditions leads to both intracellular and extracellular clustering of the particles.(Figure 13 B, C; black arrows). Intracellular endosomal clustering is observed in all 1,5µg/ml PLL samples regardless of the applied Endorem® concentration

(Figure 13 D-F; black arrows). Extracellular clustering was only observed in the 1,5µg/ml PLL – 15µg/ml or 50µg/ml Endorem® conditions (Figure 13 D, F). Based on these results, labelling conditions using 50µg/ml Endorem® led to ubiquitous endosomal clustering and were therefore left out of consideration in subsequent MTT and cellular iron determination experiments.

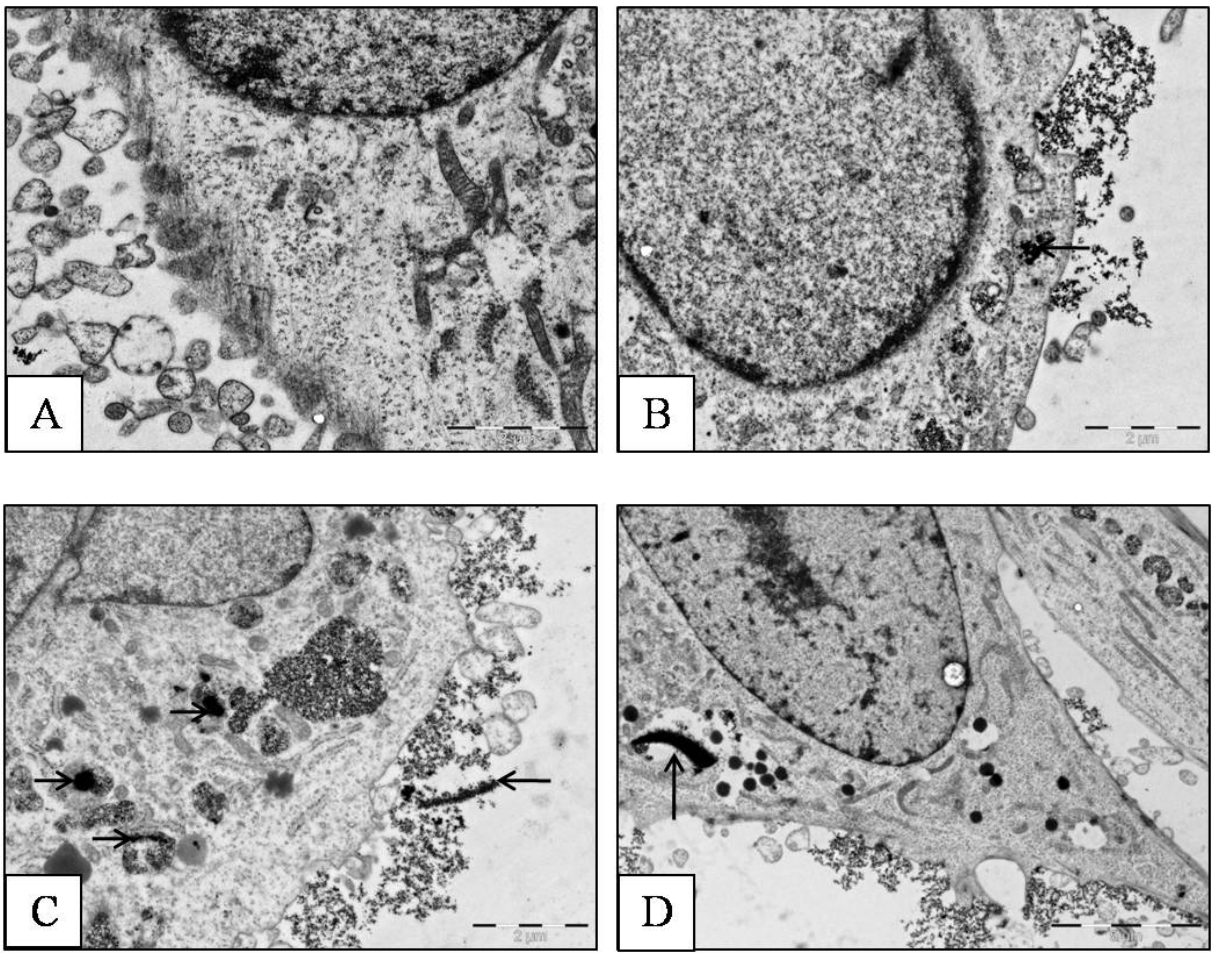

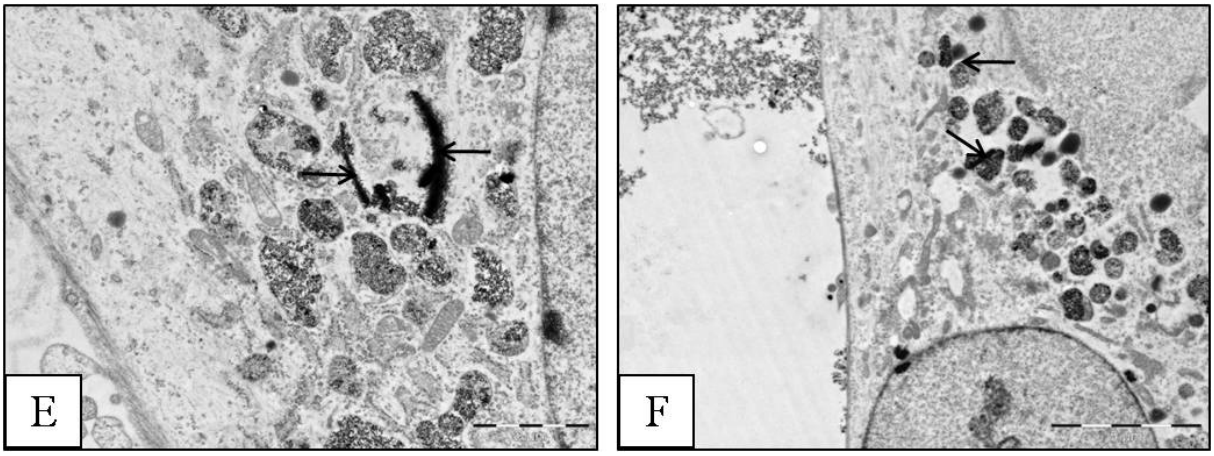

Figure 13: EM analysis of DPSCs 3 days after PLL/Endorem® labelling. Compared to controls (A), the addition of either 0,75µg/ml PLL with 25µg/ml or 50µg/ml Endorem® (B and C respectively) or 1,5µg/ml PLL with 15µg.ml, 25µg/ml or 50µg/ml Endorem® (D-F respectively) did not alter cellular morphology. Intracellular endosomal clustering of Endorem® particles is observed in all conditions, (B-F; black arrows). Extracellular clustering is observed in all labelled samples except for the 1,5µg/ml PLL – 25µg/ml Endorem® condition (B-D, F). (Scale bars: A-C, E= 2µm; D, F= 5µm)

3.7 MTT assay of Poly-L-Lysine/Endorem® labelled DPSCs

Three days after labeling DPSCs with different conditions of PLL/Endorem®, an MTT assay is performed to evaluate cell viability/metabolic activity (Figure 14). All data are compared with the 0µg/ml PLL/ 0µg/ml Endorem® condition, which is defined as 100% metabolic activity. 10% DMSO is used as a control for cell death. The addition of PLL in 0,75µg/ml or 1,5µg/ml does not significantly alter metabolic activity, nor does the addition of 15µg/ml or 25µg/ml Endorem® in the absence of PLL. However, adding 0,75µg/ml PLL to 15µg/ml Endorem® does significantly alter relative metabolic activity. Increasing the iron content in the 0,75µg/ml PLL condition does not lead to any significant changes in metabolic activity compared to the 0,75µg/ml-15µg/ml Endorem® situation. Combining 1,5µg/ml PLL with 15µg/ml Endorem® does not have a significant effect on relative metabolic activity. Higher concentrations of Endorem® (25µg/ml) with 1,5µg/ml do lead to significant differences in relative metabolic activity. Data are checked for normality with a D'Agostino and Pearson test followed by a one way ANOVA analysis and a Tukey post test. Data are represented as S.E.M. and a p-value of $\leq 0,05$ is considered statistically significant.

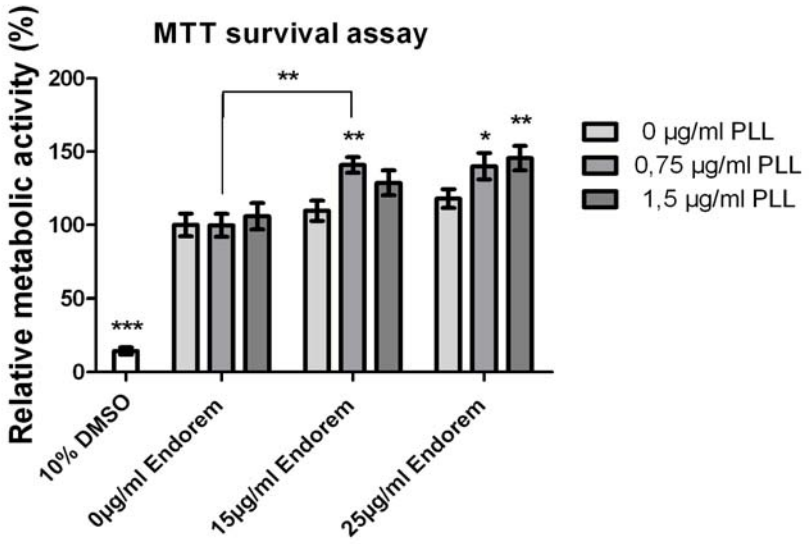

Figure 14: MTT assay results after PLL/Endorem® labelling of DPSCs. Relative metabolic activity is defined by comparing different experimental groups with the control samples (0µg/ml PLL – 0µg/ml Endorem®) which are defined as 100% metabolic activity. The addition of 0,75µg/ml or 1,5µg/ml PLL does not significantly alter relative metabolic activity, nor does the addition of 15µg/ml, 25µg/ml in the absence of PLL. Combining 0,75µg/ml PLL with 15µg/ml Endorem® does significantly increase relative metabolic activity. Combining 1,5µg/ml PLL with 15µg/ml of Endorem® does not lead to a significant increase in relative metabolic activity. Data were analyzed with one way ANOVA followed by a Tukey post test and are represented as S.E.M; * = p-value ≤ 0,05; ** = p-value ≤ 0,01; *** = p-value ≤ 0,001.

3.8 Intracellular iron content determination of Poly-L-Lysine/Endorem® labelled DPSCs

The cellular iron content after labelling with PLL and Endorem® was determined using AAS three days after labelling. These results are presented in Figure 15. Data are represented as relative increases in iron content, compared to the control condition of 0µg/ml PLL – 0µg/ml Endorem®. With equal amounts of PLL there is a dose-response relationship between conditions with different iron content ranging from 0µg/ml to 25 µg/ml. However, these results are not uniformly statistically significant as the addition of 15µg/ml Endorem® to 1,5µg/ml PLL does not lead to a significant increase in relative iron content. Increasing the Endorem® concentration from 0 to 15µg/ml in the presence of 0,75µg/ml PLL leads to a significant increase in relative iron content. A p-value ≤ 0,05 is considered statistically significant. Data were normalized with 0% being the lowest and 100% being the highest value in the original dataset (iron content in pg/ml). A one way ANOVA test was performed followed by a Bonferroni multiple comparison post test. Coupled back to the original dataset,

the significant relative increase in iron content in 0,75µg/ml PLL – 15µg/ml Endorem® is in the range of 13,36 pg/ml (s.d = 2,53) as compared to controls.

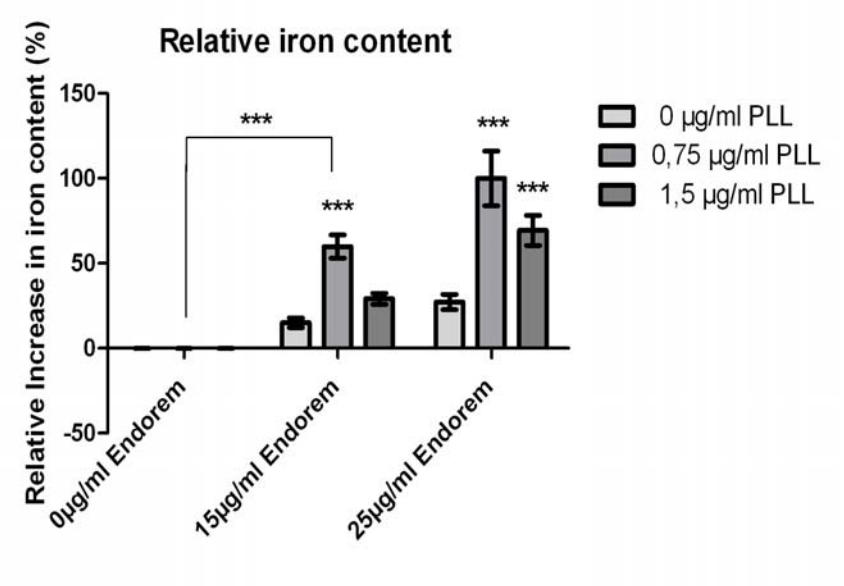

Figure 15: Intracellular iron content determination with AAS after labelling DPSCs with PLL/Endorem®. Relative increments in intracellular iron content are compared to the control condition consisting of 0µg/ml PLL and 0µg/ml Endorem®. A significant relative uptake of Endorem® particles is achieved by combining 0,75µg/ml PLL and 15µg/ml Endorem®. Combining 15µg/ml Endorem® with 1,5µg/ml PLL did not lead to a significant relative increase in iron content. The addition of 0,75µg/ml or 1,5µg/ml PLL without Endorem® did not lead to significant changes in relative iron content. Data were analyzed with one way ANOVA with a Bonferroni multiple comparison post test after normalizing the data. Data are represented as S.E.M.*= p-value ≤ 0,001**

3.9 Neurogenic differentiation of Poly-L-Lysine/Endorem® labelled DPSCs

Based on previous results, 0,75µg/ml PLL - 15µg/ml Endorem® was considered the most suitable working concentration in labelling DPSCs. Therefore, the effect of PLL-Endorem® labelling on neurogenic differentiation was assessed in a pilot experiment (n=2). Labelling of DPSCs with 0,75µg/ml PLL - 15µg/ml Endorem® did not inhibit neurosphere formation nor cellular outgrowth of differentiated DPSCs after attachment of neurospheres to coated cell culture plates (Figure 16 A,B). Differentiated cells that grew out of the neurospheres appear as bipolar cells with cytoplasmatic extensions (Figure 16C).

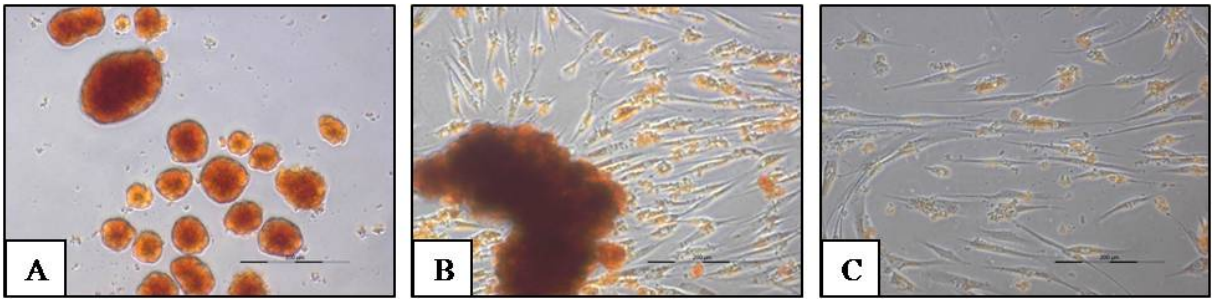

Figure 16: Phase-contrast microscopic images of DPSCs labelled with 0,75µg/ml PLL - 15µg/ml Endorem®. Labelling did not inhibit neurosphere formation nor cellular outgrowth of differentiated DPSCs after attachment of neurospheres to cell culture plates (A, B). Differentiated cells appear as bipolar cells with cytoplasmatic extensions (C). (scale bars= 200µm)

The ultrastructural evaluation of labelled differentiated DPSCs is presented in Figure 17. Labelling differentiating DPSCs with 0,75µg/ml PLL and 15µg/ml Endorem® does not influence cellular integrity as the nucleus, cellular membrane and intracellular organelles are preserved (Figure 17 A, B). Differentiated, labelled cells show a bipolar morphology and retain their metabolic activity as compared to non-labelled differentiated cells (Figure 17 A, B). The intracellular endosomal Endorem® particles are homogeneously distributed in endosomes (Figure 17 A, B; black arrows).

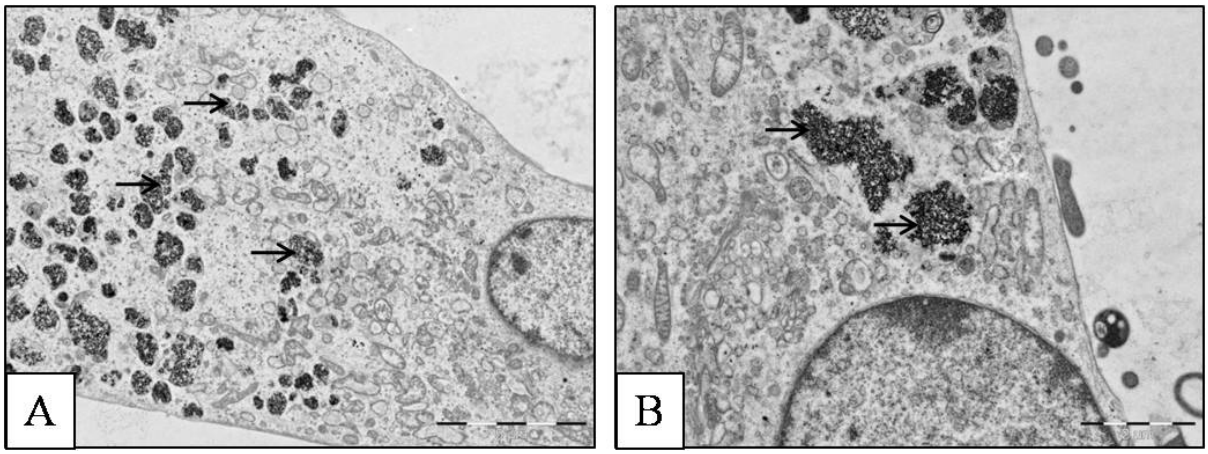

Figure 17: Ultrastructural evaluation of 0,75µg/ml PLL – 15µg/ml Endorem® labelled differentiated DPSCs. Cell morphology is preserved and differentiated, labelled cells show a bipolar morphology and retain their metabolic activity (A, B). Endorem® particles are homogeneously distributed in endosomes (A, B; black arrows). (scale bars A = 5µm: B= 2µm)

Interestingly, TEM analysis of differentiated, labelled cells showed the presence of a cilium (Figure 18; black arrow).

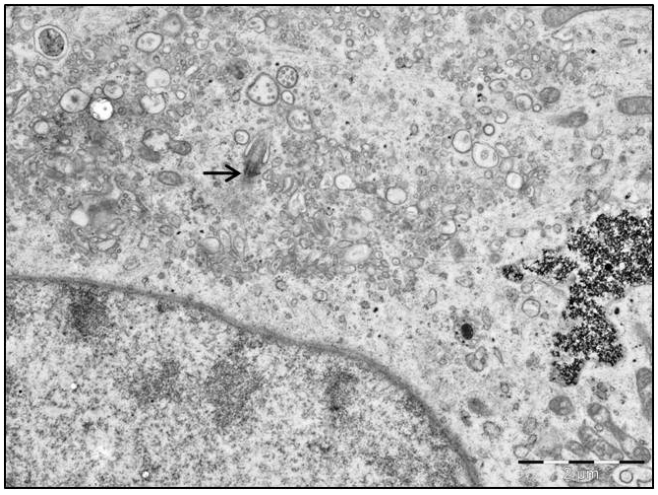

Figure 18: differentiated, labelled DPSCs showed the presence of a cilium (black arrow). (Scale bar= 2µm)

Labelled differentiated DPSCs were subjected to immunocytochemical analysis for NGFRp75 and NeuN as these markers were differentially expressed in neurogenic differentiated DPSCs compared to non differentiated DPSCs. Immunoreactivity was observed for NGFRp75, but not for NeuN (Figure 19 A and B respectively). The cytoplasmatic presence of iron deposits (black arrows) are not to be mistaken for immunoreactivity. Perls' iron staining for DPSCs labelled with 75µg/ml PLL - 15µg/ml Endorem® can be found in Supplemental data Figure S4, demonstrating iron deposits.

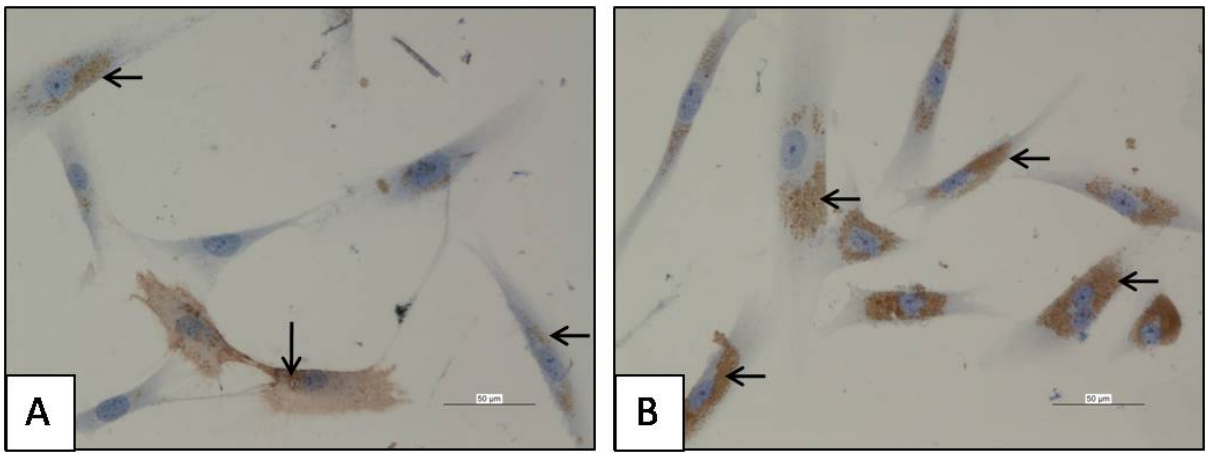

Figure 19: Immunoreactivity for 75µg/ml PLL - 15µg/ml Endorem® labelled DPSCs for the markers NGFRp75 (A) and NeuN (B). Labelled differentiated DPSCs retain immunoreactivity for NGFRp75 but immunoreactivity for NeuN could not be observed. Black arrows indicate intracellular iron deposits. (scale bars= 50µm)

4 Discussion

Prior to using MSCs as a clinical application in (neuro)degenerative diseases, thorough pre-clinical research needs to be performed. In this study, an alternative MSC source originating from the dental pulp was used rather than the conventional BMMSCs that is most widely used as an MSC model. DPSCs were successfully isolated from extracted third molars and were subjected to neural differentiation – and iron oxide nanoparticle labelling experiments.

In first instance, the immunophenotypical expression profile of DPSCs was determined. DPSCs are positive for the MSC markers CD29, CD44, CD105 and CD146 while being partially positive for CD117 and negative for the HSC marker CD34. DPSCs are also shown to be positive for vimentin, demonstrating their mesenchymal origin. However, immunoreactivity to nestin suggests that DPSC retain some neural precursor abilities. Stro-1 is proposed as a marker for a subset of MSCs reflecting more potent differentiation abilities. DPSCs show partial immunoreactivity for this marker. In a pilot experiment, the expression of these general MSC markers was compared between DPSCs and BMMSCs. BMMSCs showed a similar immunophenotypic profile for CD29, CD44, CD146, CD117, vimentin, and Stro-1. Expression of CD105 and nestin could not be detected in contrast to previous studies [42]. Furthermore, BMMSCs were partially positive for CD34. Using the proposed minimal criteria of the International Society for Cellular Therapy to define human MSC to compare the present results several conclusions and objections can be proposed [43]. The first criterion states that MSCs must be plastic adherent in standard culture conditions which was accomplished by both DPSCs and BMMSCs in the present study. Secondly, MSCs must positively express (≥95%) CD105, CD73 and CD90 while negatively expressing (≤2% positive) CD45, CD34, CD14 or CD11b, CD79α or CD19 and HLA-DR. In the present study immunoreactivity was only shown for CD105 in DPSCs and not in BMMSCs. Furthermore DPSCs demonstrated entire negativity for CD34 while BMMSCs showed partial immunoreactivity. Finally MSCs must be able to differentiate to chondroblasts, adipocytes and osteoblast *in vitro* under appropriate differentiation conditions which was previously shown in our lab for DPSCs and in multiple studies for both DPSCs and BMMSCs [10, 14, 15].

As each lab has its own methods of determining MSC properties of their used cell subjects, the proposition of the International Society for Cellular Therapy can greatly improve interlaboratory consent of both applied cell cultures and the subsequent results. It can

therefore be proposed to evaluate the expression of the proposed markers in DPSCs to gain a more stable and generally approved stem cell population. However, a study by Laino et al. shows expression of CD117 and CD34 in a specific subset of DPSCs, while a study by Kaiser at al. demonstrates the same for BMMSCs [44, 45]. To what extent the presence of these subtypes can influence MSC characteristics –if there is any- needs to be determined. Furthermore, the suggestion of using Stro-1 as a marker for more potent MSCs capable of multilineage differentiation potential needs to be clarified. One approach could comprise using a specific gene expression analysis for adipogenic, chondrogenic, osteogenic and neurogenic associated genes, comparing Stro-1^+ to Stro-1^- cells [30].

Immunocytochemical analysis of DPSCs for neural related genes shows basal expression of beta-III tubulin, S-100, synaptophysin, NSE, GalC, A2B5 and partial expression of neurofilament and NGFRp75. Basal expression could not be observed for GFAP, PGP9.5, NCAM and NeuN. BMMSCs showed a comparable basal immunoreactivity for the suggested markers, except for NSE which was only partially expressed and neurofilament for which no expression could be observed. Studies discussing basal expression of neural associated markers are scarce, focussing on the expression after differentiation. Studies that have done so mainly focussed on BMMSCs [42, 46]. An additional study has found interdonor variability in selected markers potentially influencing experimental outcomes [47]. Reports on basal marker expression in DPSCs are limited [20, 21]. Perivascular expression of neurofilament, S-100 and NSE could be observed in the dental pulp [48]. Therefore, critical interpretation of reported neural associated marker expression following differentiation needs to be kept in mind as even basal expression of neural associated markers is subjected to interdonor variability.

Subjecting DPSCs to neurogenic differentiation using EGF and bFGF as inducing agents leads to neurosphere formation when cultured in low attachment well plates. After subsequent neurosphere transfer and cell outgrowth, ultrastructural analysis of differentiated DPSCs show a more cellular distribution of cell organelles as compared to their non-differentiated counterparts where cell organelles are distributed more perinuclear. In addition, elongation of cellular processes and a more bipolar morphology is observed. Metabolic activity seems to be increased in differentiated cells, based on a more prominent Golgi-apparatus and intracellular vesicular activity. At cell-cell contact zones, vesicular release between cells is observed. Whether these vesicles contain neurotransmitters is a topic that needs further attention. Using immuno-EM, the content of these vesicles can be evaluated.

Repeating the immunocytochemical analysis of the proposed neural associated markers in differentiated DPSC demonstrates an apparent increase in immunoreactivity to NGFRp75 as both the staining intensity and number of NGFRp75 positive cells seems to be increased. The only marker for which a clear increase in reactivity was observed is NeuN. Differentiated cells were positive for beta III-tubulin, S-100, synaptophysin, NSE, GalC, A2B5 and partial expression for neurofilament was observed, but this was indistinguishable from undifferentiated cells. Neurogenic differentiation did not lead to an increased response for GFAP, PGP9.5 and NCAM, in contrast with present literature [15, 20, 23]. The lack of NCAM-expression may be attributed to the failure of differentiated cells to form stable intercellular connections. Failure to observe GFAP, PGP9.5 and NCAM expression can have multiple reasons. Expression of NeuN but not GFAP might indicate a tendency to differentiate towards neuronal cells instead of glial cells. Another cause might be the incubation time of differentiation DPSCs as this incubation time varies between different studies which might have an effect on neurogenic properties of differentiating DPSCs [17, 20, 21]. A final motive for the inconsistent results might be accounted to the heterogeneous cell population that is present in the dental pulp which form neurospheres *in vitro*. While Stro-1 and NGFRp75 positive cells might be proposed as a source of potent cells with more multilineage differentiation potential, the small fractions of DPSCs positive for either of two markers varies significantly among the FACS analyzed samples. While Stro-1 is suggested as a general marker for more potent cells, NGFRp75 is implied as a specific marker for neural crest derived cells potentially showing more predisposition to neural differentiation.

It is assumed that the dental pulp is of ectomesenchymal origin, being constituted of neural crest derived ectoderm and mesenchym. Due to genetic reprogramming, neural crest derived cells become committed to a specific cell type in the tooth or dental pulp, thereby losing specific markers to isolate these cells from the total cell population [49]. NGFRp75 expression is maintained in a subset of cells making FACS isolation of these cells a considerable approach in neurogenic differentiation experiments. Not only the tooth is comprised of neural crest derived cells, as these cells are also found in the bone marrow and the fractions of cells positive for NGFRp75 in each sample population needs to be determined [50]. Stochastically, the chances of selecting NGFRp75 positive cells for neurosphere formation are minimal. This is another argument for sorting the NGFRp75 positive fraction of DPSCs out of an entire population. Another argument in sorting DPSCs is that there is no uniform opinion on neurosphere generation. Studies arguing with the use of neurospheres as a

method for neurogenic differentiation state that neurospheres are not clonogenic. Arguments include that neurospheres are comprised of the fusion of diverse neurospheres with possible different characteristics influencing the micro-environment of both fused neurospheres creating diversity in differentiational outcome [51].

Another approach in improving the success-rate of neurogenic differentiation of DPSCs is activating specific differentiation pathways. For neurogenic differentiation in DPSCs, the protein kinase C and cyclic adenosine monophosphate pathways have been proposed while the protein kinase A pathway had previously been described for BMMSCs [21, 52]. Therefore, concentrating on pathway analysis and activating specific molecules in these pathways might lead to more successful differentiation experiments.

Nonetheless a more quantitative approach is recommended for all proposed markers, including those that are upregulated by neurogenic differentiation. This can gain more insight in both expression levels as positive cell fractions for the selected markers. Comparing basal expression of neural associated markers with the expression level after differentiation can give additional information of marker expression, in contrast to basic immunocytochemical analysis. Using quantitative polymerase chain reaction the expression level can be quantitatively determined while FACS analysis can be used to determine positive cell fractions in the applied DPSC population. Neither of these approaches can demonstrate true functionality of the differentiated cells. Therefore, additional studies should include electrophysiological patch clamp experiments to determine the potential of differentiated cells to generate an action potential. Even if the presence of an action potential cannot be detected, the occurrence of inward sodium currents or outward potassium currents can give functional information of the differentiated cells.

MRI images of 24 hour and three day- PLL/Endorem® labelled DPSCs, show that the addition of PLL is required to improve contrast in MRI scans. Increasing the Endorem® concentration from 15µg/ml to 25µg/ml and 50µg/ml in the presence of either 0,75µg/ml or 1,5µg/ml PLL does not lead to an additional increase in contrast (or decrease in relative signal intensity). As the addition of PLL significantly increased contrast in MRI images compared to PLL free labelling conditions, those lacking PLL were left out of consideration. Adding 0,75µg/ml PLL to 15µg/ml Endorem® led to an increase in contrast in MRI images both 24 hours and three days post-labelling. However, a significant difference in relative signal intensity was observed 24 hours and three days after labelling. This can be attributed to a persistence of cell proliferation after cell-labelling, dividing the endocytosed Endorem® particles between

proliferating cells. A division of Endorem® particles leads to a decrease in the amount of Endorem® in the cell, rendering the decrease in relative signal intensity less pronounced. Nonetheless, this concentration was able to significantly alter relative signal intensity to the extent that labelled DPSCs were visualized in MRI scans. Therefore, the influence of this labelling condition on cellular morphology was evaluated in addition to the intracellular distribution in the particles. These results showed that both 24 hours and three days post-labelling, cellular morphology was preserved and that the Endorem® particles were homogeneously distributed in endosomes. MRI images three days post-labelling show that labelling DPSCs with Endorem® concentrations ranging from 15µg/ml to 25µg/ml and 50µg/ml in the presence of either 0,75µg/ml or 1,5µg/ml PLL led to an increase in contrast. Therefore the intracellular distribution of Endorem® particles 3 days after labelling was evaluated in Endorem® concentrations ranging from 25µg/ml and 50µg/ml in the presence of 0,75µg/ml PLL or 15µg/ml, 25µg/ml and 50µg/ml Endorem® with 1,5µg/ml PLL. As controls, 0µg/ml PLL – 0µg/ml Endorem® samples were used. In all labelling conditions cell morphology was preserved and the intracellular uptake of iron was observed. Based on this ultrastructural analysis, labelling of DPSCs with 50µg/ml Endorem® and either 0,75µg/ml or 1,5µg/ml led to a drastic increase in intracellular endosomal clustering of the Endorem® particles. Compared to the 0,75µg/ml PLL - 15µg/ml Endorem® condition, the other labelling concentrations led to an increase in intracellular endosomal clustering of the Endorem® particles. Based on their increased tendency to form intracellular clustered beads, conditions using 50µg/ml Endorem® were left out of consideration in subsequent experiments. The MTT results suggest an increase in relative metabolic activity in PLL/Endorem® labelled DPSCs compared to controls. However, the labelling condition comprised of 15µg/ml/ Endorem® with 1,5µg/ml PLL did not lead to significant increases in metabolic activity. The term metabolic activity is more appropriate to be used as metabolic active, viable cells, are responsible for the MTT signal. An increase in mitochondrial activity could therefore be responsible for the increase in metabolic activity as supported by several studies that assign this increase in metabolic activity to the production of reactive oxygen species (ROS). These studies suggest that labelling cells with dextran coated ferumoxides leads to an increased intracellular ROS concentration, affecting the metabolic activity in the mitochondria of viable cells. This altered metabolic activity might influence the outcome and interpretation of the MTT assay. However, studies using rat macrophages and iron oxide based nanoparticles describe this effect to be transient and not affecting cell viability [53-55]. Determining the

intracellular iron content following PLL/Endorem® labelling shows a significant relative increase in intracellular iron content when compared to the non-labelled controls. However, this significant increase could not be observed in the 1,5µg/ml PLL -15µg/ml/ Endorem® possibly explaining the absence of increased relative metabolic activity. An explanation for this lack of increased relative intracellular iron content might be attributed to high extracellular clustering, not bound to DPSCs leading to a washout of the particles with each washout step. Coupling back the interpretation of the normalized dataset to the original values of intracellular iron content (pg/ml per cell) shows an intracellular iron content in the range of 10-20pg/ml per cell after labelling with 0,75µg/ml PLL - 15µg/ml Endorem®. This is consistent with the current literature in labelling MSCs [39, 56]. Several studies stress to determine the optimal labelling concentration for each cell type and labelling type [56, 57]. This study was able to determine the optimal labelling concentration of DPSCs with PLL/Endorem®. This concentration is 0,75µg/ml PLL with 15µg/ml Endorem® based on MRI, TEM, MTT and AAS analysis. Using 1,5µg/ml PLL with 15µg/ml Endorem® did not lead to increments in metabolic activity based on MTT tests while showing adequate visualization in MRI images. However, ultrastructurally this concentration is not preferred, based on intracellular endosomal clustering of the iron particles. Furthermore the increase in intracellular iron content was not considered to be significant. Authors in the aforementioned studies also take extracellular clustering of particles into account when determining optimal labelling concentrations as these might affect intra- or intercellular processes or communication. Extracellular clustering was not observed in the optimal labelling condition determined by this study. However, as TEM images are 2D and represent only a fraction of one cell, and only several cells in the entire labelled cell population, these data are to be carefully interpreted. More detailed 3D reconstructions of labelled DPSCs are required to utter relevant predictions about the role of extracellular clustering in determining the optimal labelling concentration.

In a final pilot study, the effect of labelling DPSCs with 0,75µg/ml PLL and 15µg/ml Endorem® on neurogenic differentiation of DPSCs was evaluated. PLL/Endorem® labelled cells were able to form neurospheres *in vitro* and subsequently, cellular outgrowth was observed when neurospheres attached to cell culture plates. Ultrastructurally, differentiated, labelled cells acquire a bipolar morphology and retain their metabolic activity comparable to non-labelled differentiated cells. Furthermore, a homogeneous intracellular endosomal distribution of the iron particles is observed. The presence of cilia in differentiated cells might

indicate quiescence, favouring commitment of differentiated cells to a specific cell type [58]. Immunocytochemical analysis of labelled, differentiated DPSCs shows that immunoreactivity to NGFRp75, but not NeuN is preserved. The failure to detect NeuN responsiveness might either be attributed to the labelling interfering with intracellular differentiation processes or either to the beforementioned heterogeneity in DPSCs and the critical view towards neurosphere formation. In conclusion, it can be concluded that labelling DPSCs does not influence neurosphere formation and subsequent cellular outgrowth. Endorem® particles are retained in the cells following differentiation and are distributed homogeneously while preserving cellular morphology. Immunoreactivity for NGFRp75 is preserved in contrast to NeuN.

As exact therapeutic options with MSCs or DPSCs are not yet available, a broad analysis of possible applications needs to be taken into account. Tissue replacement by stem cell transplantation is one of the possible applications in stem cell research. Others include modulation of the microenvironment both immunologically or by the release of several (neuro)trophic factors. Furthermore it has been shown that MSCs have a tropism for wounding and tumor micro-environments, but the precise mechanisms of action after their homing are still unknown [59]. Combining these possible applications of MSCs with PLL/Endorem® labelling can lead to applications in both degenerative medicine and tumor research as PLL/Endorem® labelling makes these cells visible following engraftment. This is not only obligatory in human applications, but also in basal research to determine stem cell fate in animal models following engraftment before human tests are even taken into consideration. For labelled DPSCs to be used clinically, the exact effect of labelling on cellular processes needs to be elucidated. Since it has been shown that dextran coated iron oxide particles such as Endorem® can increase the reactive oxygen species concentration in the cell, this can affect cellular processes. Even when general cellular processes are not affected based on long term follow-up of labelled DPSCs, the influence of PLL/Endorem® labelling on neurogenic differentiation needs to be assessed. More specifically, pathways involved in differentiation can be studied to gain more insight in affected cellular pathways. Only when the influence of Endorem® on cellular processes is sorted out, it can be considered as an intracellular imaging agent.

Taken together, this study shows high basal expression of neural associated markers in both DPSCs as BMMSCs. Differentiated DPSCs show an upregulation of NGFRp75 and NeuN.

Ultrastructurally, differentiated cells show more metabolic activity and acquire a bipolar cell morphology with cytoplasmatic extensions. Future studies should focus on more quantitative approaches in determining marker expression following differentiation and should be combined with electrophysiological tests to assess functionality of differentiated cells. DPSCs can be labelled with PLL/Endorem®, the optimal concentration being 0,75µg/ml PLL and 15µg/ml Endorem® as determined by MRI, MTT, AAS and TEM analysis. The influence of PLL/Endorem® labelling on intracellular processes and pathways needs to be elucidated for this labelling approach to be used both experimentally and clinically. In this context, the proposed hypothesis is partially covered as an appropriate marker for differentiated cells is found and it is shown that DPSCs can be labelled with the ferumoxide Endorem®.

.

Conclusion

One of the most important medical discoveries of the twentieth century was the existence of stem cells with the ability to self renew and differentiate into multiple cell types. The cells with the most outspoken differentiation potential are not available for scientific research due to ethical considerations as these cells are of embryonal origin. Therefore, stem cells from the adult organism are used in stem cell research. Stem cells are considered as a therapeutic option in untreatable diseases and most research with stem cells focuses on applications of stem cells in degenerative diseases. Degenerative disorders of the central nervous system are generally considered as untreatable and the ideal stem cell type for treating these diseases is the NSC. Unfortunately, human experiments with autologous NSC are challenging to perform due to the scarce amount of NSC in the adult brain while also being difficult to harvest. Therefore, the search for an alternative source of stem cells with neural differentiation potential is an open challenge. MSCs have already shown to retain some plasticity to differentiate into neural cells. The most uniformly used type of MSC is the BMMSC. However, isolation of BMMSCs is a painful procedure with high donor site morbidity. Recently, alternative -more accessible- sources of MSCs have been discovered including the umbilical cord, adipose tissue and the tooth. This study focused on the stem cells isolated from the human dental pulp (DPSCs). As these cells were already shown to share some characteristics with BMMSCs, the basal expression of conventionally used neural related markers was compared between these two cell types with prospect on neural differentiation of DPSCs. The basal expression of neural related markers was comparable between both cell types, except for neurofilament and nestin which were not found to be expressed in BMMSCs and NSE which was differentially expressed in BMMSCs compared to DPSCs. The lack of immunoreactivity of BMMSCs to nestin is in contrast with the current literature. This can be attributed to interdonor variability for neural associated markers. Differentiated DPSCs showed upregulation of NGFRp75 and NeuN, although only partially for NGFRp75. These results stress the importance of specific markers to distinguish between differentiated and undifferentiated cells as most markers that showed immunoreactivity are used in various studies to show neurogenic differentiation. However, more quantitative measurements of marker expression with quantitative polymerase chain reaction can be used to check upregulation of neural associated markers following differentiation. As NGFRp75 is considered as a marker for neural crest derived cells, the fraction of DPSCs positive for this marker was assessed with FACS together with the percentage of Stro-1, another marker for

potent MSCs regarding multilineage differentiation potential. Results show high variability between the different observed samples highlighting the heterogeneity of DPSCs. Sorting DPSCs for NGFRp75 to evaluate neurogenic differentiation potential of these cells is a future option that has to be taken into account. Ultrastructurally, differentiated cells show increased metabolic activity based on the presence of vesicular transport both within and between cells. Whether the intercellular released vesicles contain neurotransmitters is a question that remains to be addressed using for example immuno electron microscopy.

In a second part of the present study, DPSCs were labelled with the commercially available ferumoxide Endorem® combined with PLL in order to determine the optimal labelling concentration of this cell type. This concentration was shown to be 0,75µg/ml PLL with 15µg/ml Endorem® based on MRI, MTT, TEM and AAS analyses. Ultrastructurally, the iron oxide particles are present as a homogeneously distributed substance in endosomes. Labelling DPSCs with this labelling concentration prior to neural differentiation experiments did not inhibit neurosphere formation and subsequent cellular outgrowth. Ultrastructurally, the morphology of differentiated DPSCs is preserved. Endorem® particles are homogeneously distributed in endosomes. An immunocytochemical analysis shows immunoreactivity for labelled cells to NGFRp75 but not for NeuN. The failure to recreate NeuN reactivity can either be attributed to the argument that neurospheres are not clonogenic units and that there are more potent DPSCs present in the total DPSCs that were not selected for neurosphere generation during the onset of the experiment. Another argument is that due to intracellular reactive oxygen production as a result of the Endorem® labelling, differentiation cascades in the cell are disrupted.

In conclusion, DPSCs are a valuable alternative MSC source for BMMSCs in neurogenic differentiation research. However, this study shows the need of a specific marker for neurogenic differentiated cells as DPSCs and BMMSCs show baseline expression of conventionally used markers. NeuN is proposed as a suitable marker to distinguish between differentiated and non-differentiated DPSCs. Future studies should include quantitative measurements of marker expression and electrophysiological experiments. Furthermore, it was shown that DPSCs can be labelled with Endorem® with 0,75µg/ml PLL - 15µg/ml Endorem® being the optimal concentration. Cell-labelling did not influence cellular morphology and Endorem® particles are distributed homogeneously in endosomes. The influence of Endorem® labelling on cellular processes needs to be determined before these cells can be considered as a clinical applicable intracellular contrast agent for MRI analysis.

References

1. Weissman IL. Stem cells: units of development, units of regeneration, and units in evolution. Cell. 2000 Jan 7;100(1):157-68.

2. Wagers AJ, Weissman IL. Plasticity of adult stem cells. Cell. 2004 Mar 5;116(5):639-48.

3. Hobbs JR. Bone marrow transplantation for inborn errors. Lancet. 1981 Oct 3;2(8249):735-9.

4. Lee KD. Applications of mesenchymal stem cells: an updated review. Chang Gung Med J. 2008 May-Jun;31(3):228-36.

5. Pluchino S, Martino G. The therapeutic use of stem cells for myelin repair in autoimmune demyelinating disorders. J Neurol Sci. 2005 Jun 15;233(1-2):117-9.

6. Slavin S, Kurkalli BG, Karussis D. The potential use of adult stem cells for the treatment of multiple sclerosis and other neurodegenerative disorders. Clin Neurol Neurosurg. 2008 Nov;110(9):943-6.

7. Moraleda JM, Blanquer M, Bleda P, Iniesta P, Ruiz F, Bonilla S, et al. Adult stem cell therapy: dream or reality? Transpl Immunol. 2006 Dec;17(1):74-7.

8. Nauta AJ, Fibbe WE. Immunomodulatory properties of mesenchymal stromal cells. Blood. 2007 Nov 15;110(10):3499-506.

9. Friedenstein AJ. Osteogenetic activity of transplanted transitional epithelium. Acta Anat (Basel). 1961;45:31-59.

10. Gronthos S, Mankani M, Brahim J, Robey PG, Shi S. Postnatal human dental pulp stem cells (DPSCs) in vitro and in vivo. Proc Natl Acad Sci U S A. 2000 Dec 5;97(25):13625-30.

11. Zuk PA, Zhu M, Ashjian P, De Ugarte DA, Huang JI, Mizuno H, et al. Human adipose tissue is a source of multipotent stem cells. Mol Biol Cell. 2002 Dec;13(12):4279-95.

12. Erices A, Conget P, Minguell JJ. Mesenchymal progenitor cells in human umbilical cord blood. Br J Haematol. 2000 Apr;109(1):235-42.

13. Decup F, Six N, Palmier B, Buch D, Lasfargues JJ, Salih E, et al. Bone sialoprotein-induced reparative dentinogenesis in the pulp of rat's molar. Clin Oral Investig. 2000 Jun;4(2):110-9.

14. Pittenger MF, Mackay AM, Beck SC, Jaiswal RK, Douglas R, Mosca JD, et al. Multilineage potential of adult human mesenchymal stem cells. Science. 1999 Apr 2;284(5411):143-7.

15. Gronthos S, Brahim J, Li W, Fisher LW, Cherman N, Boyde A, et al. Stem cell properties of human dental pulp stem cells. J Dent Res. 2002 Aug;81(8):531-5.

16. Shi S, Robey PG, Gronthos S. Comparison of human dental pulp and bone marrow stromal stem cells by cDNA microarray analysis. Bone. 2001 Dec;29(6):532-9.

17. Sasaki R, Aoki S, Yamato M, Uchiyama H, Wada K, Okano T, et al. Neurosphere generation from dental pulp of adult rat incisor. Eur J Neurosci. 2008 Feb;27(3):538-48.

18. Stevens A, Zuliani T, Olejnik C, LeRoy H, Obriot H, Kerr-Conte J, et al. Human dental pulp stem cells differentiate into neural crest-derived melanocytes and have label-retaining and sphere-forming abilities. Stem Cells Dev. 2008 Dec;17(6):1175-84.

19. Knecht AK, Bronner-Fraser M. Induction of the neural crest: a multigene process. Nat Rev Genet. 2002 Jun;3(6):453-61.

20. Arthur A, Rychkov G, Shi S, Koblar SA, Gronthos S. Adult human dental pulp stem cells differentiate toward functionally active neurons under appropriate environmental cues. Stem Cells. 2008 Jul;26(7):1787-95.

21. Kiraly M, Porcsalmy B, Pataki A, Kadar K, Jelitai M, Molnar B, et al. Simultaneous PKC and cAMP activation induces differentiation of human dental pulp stem cells into functionally active neurons. Neurochem Int. 2009 Sep;55(5):323-32.

22. Nosrat IV, Widenfalk J, Olson L, Nosrat CA. Dental pulp cells produce neurotrophic factors, interact with trigeminal neurons in vitro, and rescue motoneurons after spinal cord injury. Dev Biol. 2001 Oct 1;238(1):120-32.

23. Nosrat IV, Smith CA, Mullally P, Olson L, Nosrat CA. Dental pulp cells provide neurotrophic support for dopaminergic neurons and differentiate into neurons in vitro; implications for tissue engineering and repair in the nervous system. Eur J Neurosci. 2004 May;19(9):2388-98.

24. Apel C, Forlenza OV, de Paula VJ, Talib LL, Denecke B, Eduardo CP, et al. The neuroprotective effect of dental pulp cells in models of Alzheimer's and Parkinson's disease. J Neural Transm. 2009 Jan;116(1):71-8.

25. Huang AH, Snyder BR, Cheng PH, Chan AW. Putative dental pulp-derived stem/stromal cells promote proliferation and differentiation of endogenous neural cells in the hippocampus of mice. Stem Cells. 2008 Oct;26(10):2654-63.

26. Lovschall H, Tummers M, Thesleff I, Fuchtbauer EM, Poulsen K. Activation of the Notch signaling pathway in response to pulp capping of rat molars. Eur J Oral Sci. 2005 Aug;113(4):312-7.

27. Shi S, Gronthos S. Perivascular niche of postnatal mesenchymal stem cells in human bone marrow and dental pulp. J Bone Miner Res. 2003 Apr;18(4):696-704.

28. Zannettino AC, Paton S, Arthur A, Khor F, Itescu S, Gimble JM, et al. Multipotential human adipose-derived stromal stem cells exhibit a perivascular phenotype in vitro and in vivo. J Cell Physiol. 2008 Feb;214(2):413-21.

29. Gronthos S, Graves SE, Ohta S, Simmons PJ. The STRO-1+ fraction of adult human bone marrow contains the osteogenic precursors. Blood. 1994 Dec 15;84(12):4164-73.

30. Yang X, Zhang W, van den Dolder J, Walboomers XF, Bian Z, Fan M, et al. Multilineage potential of STRO-1+ rat dental pulp cells in vitro. J Tissue Eng Regen Med. 2007 Mar-Apr;1(2):128-35.

31. Stemple DL, Anderson DJ. Isolation of a stem cell for neurons and glia from the mammalian neural crest. Cell. 1992 Dec 11;71(6):973-85.

32. Bannerman P, Nichols W, Puhalla S, Oliver T, Berman M, Pleasure D. Early migratory rat neural crest cells express functional gap junctions: evidence that neural crest cell survival requires gap junction function. J Neurosci Res. 2000 Sep 15;61(6):605-15.

33. Waddington RJ, Youde SJ, Lee CP, Sloan AJ. Isolation of distinct progenitor stem cell populations from dental pulp. Cells Tissues Organs. 2009;189(1-4):268-74.

34. Mark B, Richard S, Thomas KN. MRI: Basic Principles and Applications, 3rd edition. Medical Physics. 2004;31(1):170.

35. Himmelreich U, Dresselaers T. Cell labeling and tracking for experimental models using magnetic resonance imaging. Methods. 2009 Jun;48(2):112-24.

36. Cohen ME, Muja N, Fainstein N, Bulte JW, Ben-Hur T. Conserved fate and function of ferumoxides-labeled neural precursor cells in vitro and in vivo. J Neurosci Res. Apr;88(5):936-44.

37. Zhu J, Zhou L, XingWu F. Tracking neural stem cells in patients with brain trauma. N Engl J Med. 2006 Nov 30;355(22):2376-8.

38. Politi LS, Bacigaluppi M, Brambilla E, Cadioli M, Falini A, Comi G, et al. Magnetic-resonance-based tracking and quantification of intravenously injected neural stem cell accumulation in the brains of mice with experimental multiple sclerosis. Stem Cells. 2007 Oct;25(10):2583-92.

39. Frank JA, Miller BR, Arbab AS, Zywicke HA, Jordan EK, Lewis BK, et al. Clinically applicable labeling of mammalian and stem cells by combining superparamagnetic iron oxides and transfection agents. Radiology. 2003 Aug;228(2):480-7.

40. Yocum GT, Wilson LB, Ashari P, Jordan EK, Frank JA, Arbab AS. Effect of human stem cells labeled with ferumoxides-poly-L-lysine on hematologic and biochemical measurements in rats. Radiology. 2005 May;235(2):547-52.

41. Farrell E, Wielopolski P, Pavljasevic P, van Tiel S, Jahr H, Verhaar J, et al. Effects of iron oxide incorporation for long term cell tracking on MSC differentiation in vitro and in vivo. Biochem Biophys Res Commun. 2008 May 16;369(4):1076-81.

42. Bertani N, Malatesta P, Volpi G, Sonego P, Perris R. Neurogenic potential of human mesenchymal stem cells revisited: analysis by immunostaining, time-lapse video and microarray. J Cell Sci. 2005 Sep 1;118(Pt 17):3925-36.

43. Dominici M, Le Blanc K, Mueller I, Slaper-Cortenbach I, Marini F, Krause D, et al. Minimal criteria for defining multipotent mesenchymal stromal cells. The International Society for Cellular Therapy position statement. Cytotherapy. 2006;8(4):315-7.

44. Laino G, d'Aquino R, Graziano A, Lanza V, Carinci F, Naro F, et al. A new population of human adult dental pulp stem cells: a useful source of living autologous fibrous bone tissue (LAB). J Bone Miner Res. 2005 Aug;20(8):1394-402.

45. Kaiser S, Hackanson B, Follo M, Mehlhorn A, Geiger K, Ihorst G, et al. BM cells giving rise to MSC in culture have a heterogeneous CD34 and CD45 phenotype. Cytotherapy. 2007;9(5):439-50.

46. Woodbury D, Schwarz EJ, Prockop DJ, Black IB. Adult rat and human bone marrow stromal cells differentiate into neurons. J Neurosci Res. 2000 Aug 15;61(4):364-70.

47. Montzka K, Lassonczyk N, Tschoke B, Neuss S, Fuhrmann T, Franzen R, et al. Neural differentiation potential of human bone marrow-derived mesenchymal stromal cells: misleading marker gene expression. BMC Neurosci. 2009;10:16.

48. Dourou V, Lyroudia K, Karayannopoulou G, Papadimitriou C, Molyvdas I. Comparative evaluation of neural tissue antigens--neurofilament protein (NF), peripherin (PRP), S100B protein (S100B), neuron-specific enolase (NSE) and chromogranin-A (CgA)--in both normal and inflamed human mature dental pulp. Acta Histochem. 2006;108(5):343-50.

49. Chai Y, Jiang X, Ito Y, Bringas P, Jr., Han J, Rowitch DH, et al. Fate of the mammalian cranial neural crest during tooth and mandibular morphogenesis. Development. 2000 Apr;127(8):1671-9.

50. Nagoshi N, Shibata S, Kubota Y, Nakamura M, Nagai Y, Satoh E, et al. Ontogeny and multipotency of neural crest-derived stem cells in mouse bone marrow, dorsal root ganglia, and whisker pad. Cell Stem Cell. 2008 Apr 10;2(4):392-403.

51. Singec I, Knoth R, Meyer RP, Maciaczyk J, Volk B, Nikkhah G, et al. Defining the actual sensitivity and specificity of the neurosphere assay in stem cell biology. Nat Methods. 2006 Oct;3(10):801-6.

52. Jori FP, Napolitano MA, Melone MA, Cipollaro M, Cascino A, Altucci L, et al. Molecular pathways involved in neural in vitro differentiation of marrow stromal stem cells. J Cell Biochem. 2005 Mar 1;94(4):645-55.

53. Soenen SJ, Brisson AR, De Cuyper M. Addressing the problem of cationic lipid-mediated toxicity: the magnetoliposome model. Biomaterials. 2009 Aug;30(22):3691-701.

54. Collier AC, Pritsos CA. The mitochondrial uncoupler dicumarol disrupts the MTT assay. Biochem Pharmacol. 2003 Jul 15;66(2):281-7.

55. Stroh A, Zimmer C, Gutzeit C, Jakstadt M, Marschinke F, Jung T, et al. Iron oxide particles for molecular magnetic resonance imaging cause transient oxidative stress in rat macrophages. Free Radic Biol Med. 2004 Apr 15;36(8):976-84.

56. Arbab AS, Bashaw LA, Miller BR, Jordan EK, Bulte JW, Frank JA. Intracytoplasmic tagging of cells with ferumoxides and transfection agent for cellular magnetic resonance imaging after cell transplantation: methods and techniques. Transplantation. 2003 Oct 15;76(7):1123-30.

57. Crabbe A, Vandeputte C, Dresselaers T, Sacido AA, Verdugo JM, Eyckmans J, et al. Effects of MRI Contrast Agents on the Stem cell Phenotype. Cell Transplant. Mar 26.

58. Rieder CL, Jensen CG, Jensen LC. The resorption of primary cilia during mitosis in a vertebrate (PtK1) cell line. J Ultrastruct Res. 1979 Aug;68(2):173-85.

59. Kidd S, Spaeth E, Dembinski JL, Dietrich M, Watson K, Klopp A, et al. Direct evidence of mesenchymal stem cell tropism for tumor and wounding microenvironments using in vivo bioluminescent imaging. Stem Cells. 2009 Oct;27(10):2614-23.

Supplemental information

S1 Supplemental materials and methods

This section contains the additional materials and methods used in this study.

S1.1 Perls' Iron staining

To visualise iron particles in Endorem® labelled cells, Perls' iron staining was used. In this staining method, potassium hexacyanoferrate (II) trihydrate ($3[Fe(CN)_6]^{4-}$) was used to react with trivalent iron particles (Fe^{3+}), forming ferri ferrocyanide ($Fe_4[Fe(CN)_6]_3$) which precipitates as Prussian blue. In order for iron to precipitate in the reaction, it needed to be present as a free Fe^{3+} ion. With the use of an acid such as hydrochloric acid (HCl), Fe^{3+} could be dissociated from cellular proteins or other Fe^{3+} containing structures.

Perls's iron staining was performed by adding equal parts of 2% HCl (Vel n.v., Heverlee, Belgium) and 2% $3[Fe(CN)_6]^{4-}$ (Vel n.v, Heverlee, Belgium) to the labelled cells for 40 minutes. After washing with distilled water, the Mayer's hematoxylin nuclear counterstain was performe. After rinsing with distilled water, the coverslips were mounted with Aquatex®.

S2 Supplemental data

In this section, the supplemental data that are referred to in the main text are listed. These data include, the morphological features and immunophenotype of BMMSCs, the basal expression of neural related markers in BMMSCs and Perls' staining of 0,75µg/ml PLL – 15 µg/ml Endorem® labelled DPSCs.

S2.1 Morphological features of BMMSCs

Morphologically, BMMSCs are radially stretched, leading to a flattened cell- morphology with multiple cellular extensions (Figure S1).

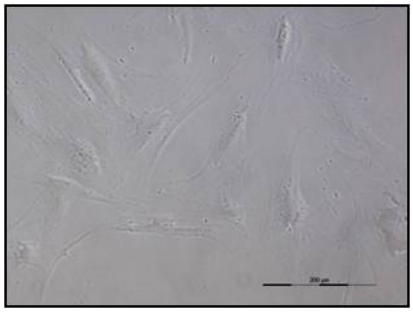

Figure S1: phase contrast image of BMMSCs in vitro demonstrating a flattened cell morphology with multiple irregularly distributed cellular extensions. (scale bar= 200µm)

S2.2 Immunophenotype of BMMSCs

The immunophenotypical analysis to evaluate mesenchymal cell properties of BMMSCs is illustrated in Figure S2. BMMSCs show immunoreactivity to CD29, CD44, CD146 and vimentin (Figure S2 A,B,D and G), but not to CD105 and nestin (Figure S2 C, I) . Slight immunoreactivity to CD34 (Figure S2 F) is observed. A fraction of BMMSCs is positive for CD117 and Stro-1(Figure S2 E and H).

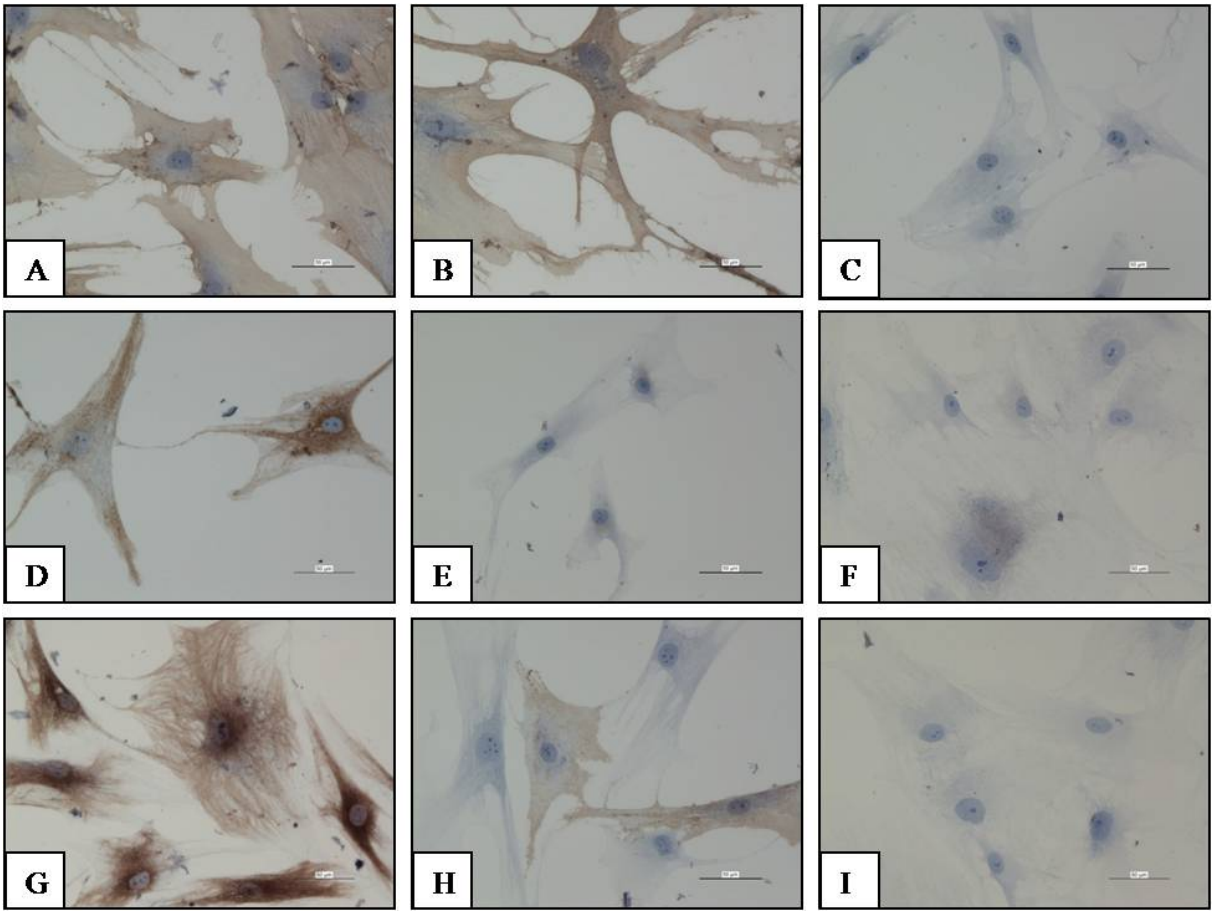

Figure S2: Immunophenotype of BMMSCs. BMMSCs show immunoreactivity for the MSC markers CD29 (A); CD44 (B), CD146 (D) and vimentin (G). Immunoreactivity for CD117 (E) and Stro-1 (H) can only be observed in a subset of BMMSCs. Immunoreactivity to CD105 (C) and nestin (I) could not be noted. Slight immunoreactivity to CD34 (F) is noticed in a small subset of BMMSCs. (Scale bars= 50µm)

S2.3 Immunocytochemical analysis of basal expression of neural related markers in BMMSCs

Basal expression of BMMSCs (n=1) was tested immunocytochemically for a variety of neural related markers. The results of this analysis are presented in Figure S3. These markers include beta-III tubulin, neurofilament, S-100, synaptophysin, NSE GalC, A2B5, GFAP, PGP9.5, NCAM, NGFRp75 and NeuN (Figure S3 A-L) respectively). Immunoreactivity was observed in beta III tubulin, S-100, synaptophysin, GalC and A2B5 (Figure S3 A, C, D, F, G). Partial immunoreactivity was shown for NSE and NGFRp75 (Figure S3 E, K).

Regarding the basal expression of the suggested markers in BMMSCs, a distinct basal immunoreactivity between DPSCs and BMMSCs was observed for neurofilament and NSE. DPSCs show a uniform reactivity against and NSE while only a fraction of DPSCs is positive for neurofilament. BMMSCs are negative for neurofilament (Figure S3B) and only a subset of BMMSCs show immunoreactivity against NSE (Figure S3E). Considering the other markers, no apparent difference in basal expression was observed as immunoreactivity in BMMSCs was observed for beta III tubulin, S-100, synaptophysin, GalC and A2B5 (Figure S3 A, C, D, F, G) while showing no expression for GFAP, PGP9.5, NCAM and NeuN (Figure S3 H-J, L). NGFRp75 (Figure S3 K) was partially expressed, comparable with DPSCs.

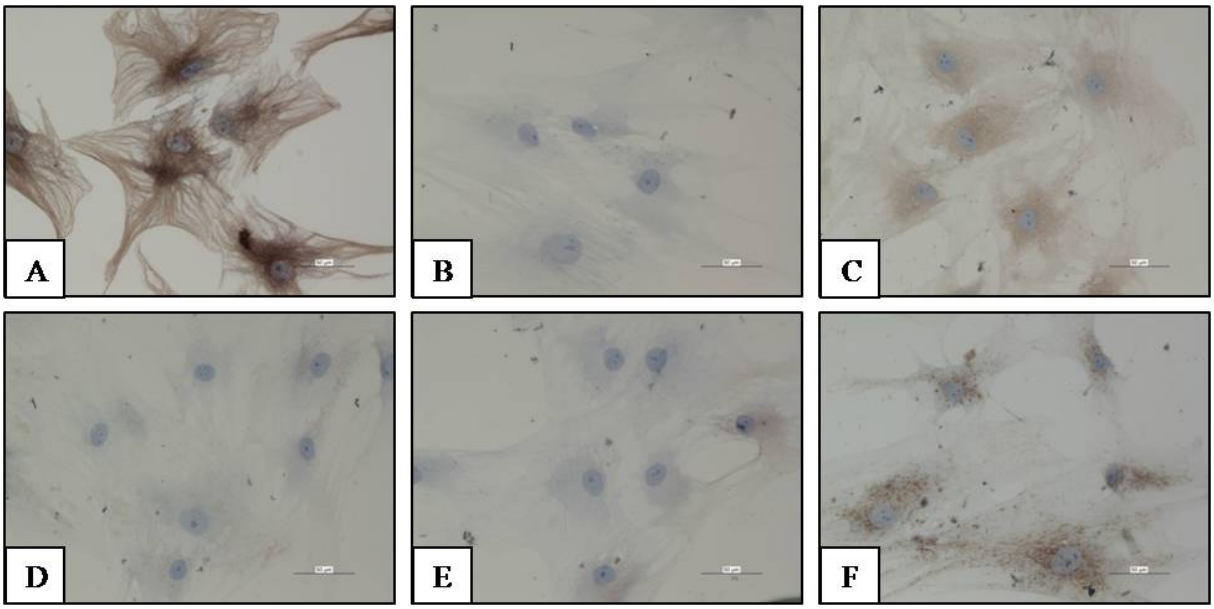

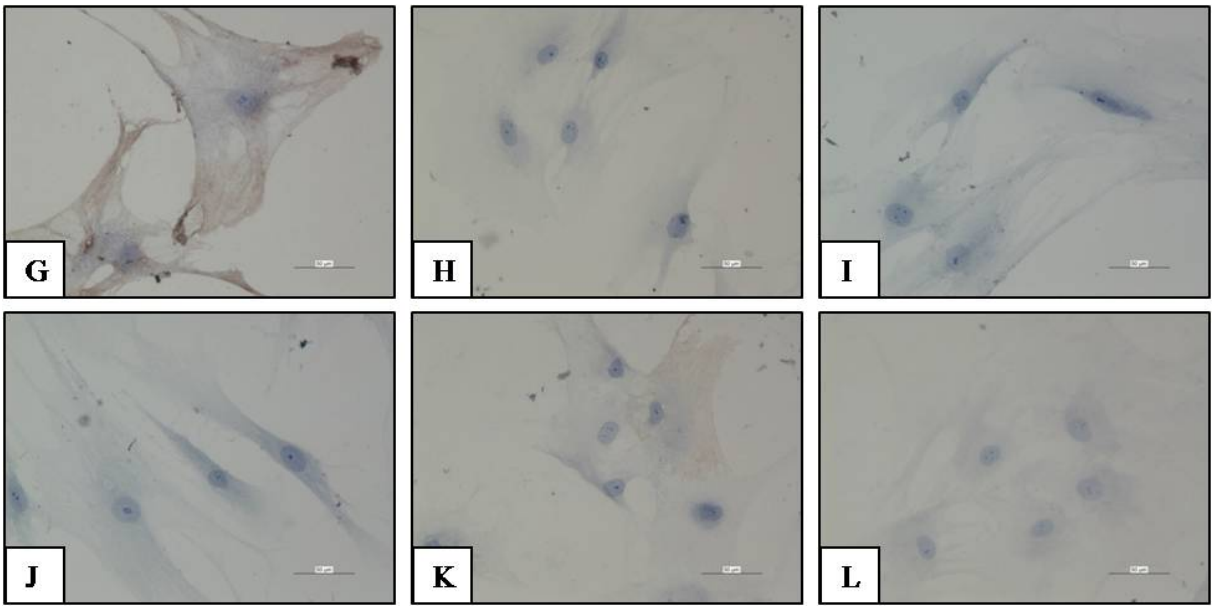

Figure S3: Basal immunoreactivity of BMMSCs to beta-III tubulin, neurofilament, S-100, synaptophysin, NSE, GalC, A2B5, GFAP, PGP9.5, NCAM, NGFRp75 and NeuN (A-L respectively). Immunoreactivity was observed in beta III tubulin, S-100, synaptophysin, NSE, GalC and A2B5. Immunoreactivity for NGFRp75 was observed in a subset of BMMSCs. (scale bars= 50µm)

S2.4 Perls' staining of 0,75µg/ml PLL – 15 µg/ml Endorem® labelled DPSCs

Using Perls' iron staining, intracellular iron deposits following Endorem® labelling can be visualized as a blue precipitation (Figure S4, black arrows). In the presented figure, Perls' staining is combined with a Ki67 proliferation marker showing active proliferation in labelled DPSCs. Ki67 shows a nuclear staining pattern.

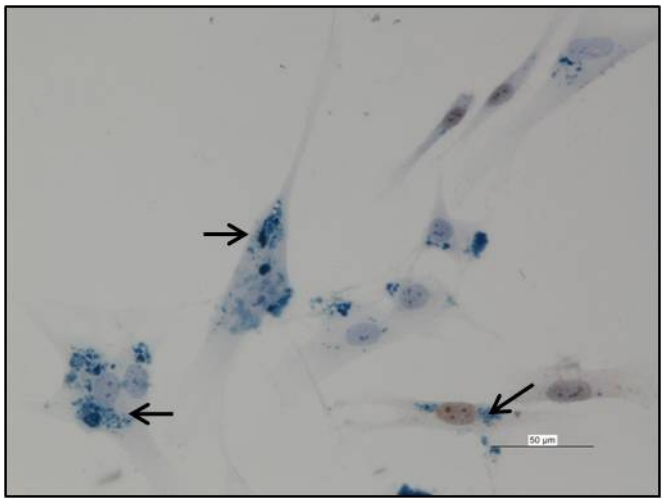

Figure S4: Perls' iron staining showing iron deposits (black arrows) in 0,75µg/ml PLL – 15µg/ml Endorem® labelled DPSCs. This Perls' staining was combined with a Ki67 staining showing nuclear immunoreactivity.

Auteursrechtelijke overeenkomst

Ik/wij verlenen het wereldwijde auteursrecht voor de ingediende eindverhandeling:
Dental pulp stem cells: neurogenic differentiation potential and ferumoxide nanoparticle labelling

Richting: **master in de biomedische wetenschappen-klinische moleculaire wetenschappen**
Jaar: **2010**

in alle mogelijke mediaformaten, - bestaande en in de toekomst te ontwikkelen - , aan de Universiteit Hasselt.

Niet tegenstaand deze toekenning van het auteursrecht aan de Universiteit Hasselt behoud ik als auteur het recht om de eindverhandeling, - in zijn geheel of gedeeltelijk -, vrij te reproduceren, (her)publiceren of distribueren zonder de toelating te moeten verkrijgen van de Universiteit Hasselt.

Ik bevestig dat de eindverhandeling mijn origineel werk is, en dat ik het recht heb om de rechten te verlenen die in deze overeenkomst worden beschreven. Ik verklaar tevens dat de eindverhandeling, naar mijn weten, het auteursrecht van anderen niet overtreedt.

Ik verklaar tevens dat ik voor het materiaal in de eindverhandeling dat beschermd wordt door het auteursrecht, de nodige toelatingen heb verkregen zodat ik deze ook aan de Universiteit Hasselt kan overdragen en dat dit duidelijk in de tekst en inhoud van de eindverhandeling werd genotificeerd.

Universiteit Hasselt zal mij als auteur(s) van de eindverhandeling identificeren en zal geen wijzigingen aanbrengen aan de eindverhandeling, uitgezonderd deze toegelaten door deze overeenkomst.

Voor akkoord,

Gervois, Pascal

Datum: **15/06/2010**